

# PROTON RADIOGRAPHY OF DENSE PLASMA

Introduction

ITEP-TWAC Facility

Detonation Studies

Dynamic Surface Ejecta

Formation

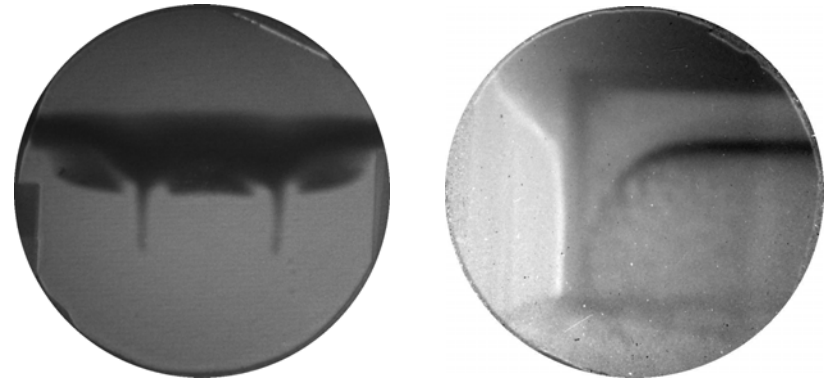
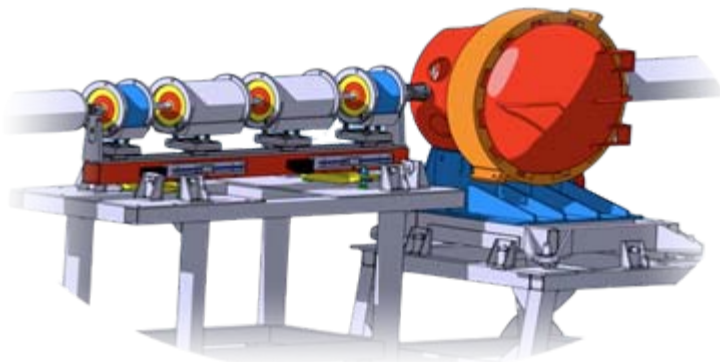
Development of Compact

Explosive Generators

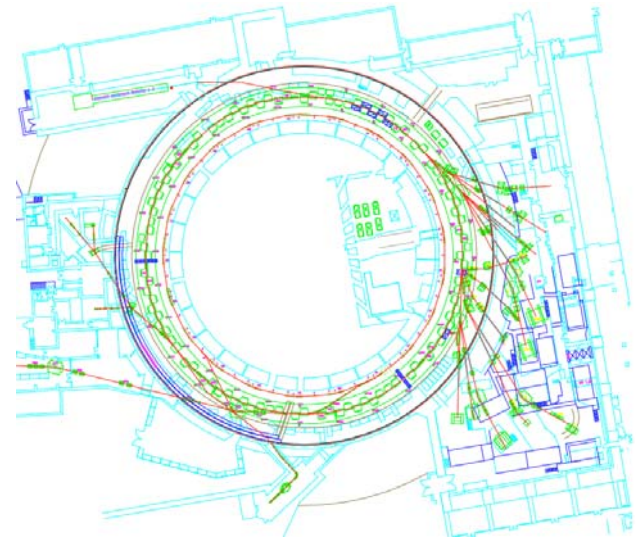
Shock Compression of

Noble Gases

Conclusions



Scientific-coordination session  
"Non-Ideal Plasma Research"  
November 23-24, 2011, Moscow



*IPCP RAS, Chernogolovka, Russia*  
*JIHT, Moscow, Russia*

V.B. Mintsev, S.A. Kolesnikov, S.V. Dudin,  
V.V.Lavrov, D.N.Nikolaev, A.V. Savchenko,  
V.Ya.Ternovoi, A.V.Utkin, N.S. Shilkin,  
D.S.Yuriev, V.E. Fortov



*ITEP, Moscow, Russia*

A.A. Golubev, K.L. Gubsky, V.S. Demidov,  
A.V.Kantsyrev, A.P. Kuznetzov, G.N.Smirnov,  
V.I.Turtikov, A.D.Fertman, L.M.Shestov,  
B.Yu.Sharkov



*RFNC – VNIIEF, Sarov, Russia*

V.V.Burtsev, N.V.Zavialov, S.A.Kartanov,  
A.L.Mikhailov, A.V.Rudnev, M.V.Tatsenko,  
M.V.Zhernokletov



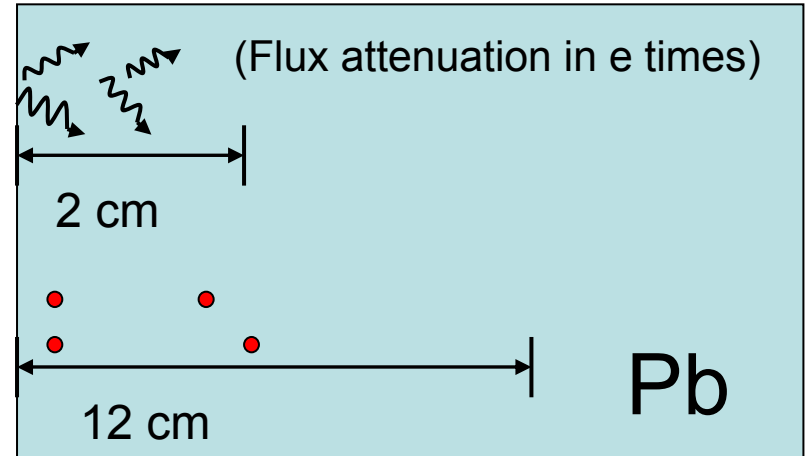
# Radiography Basics

## Photons and charged particles in matter

X-rays 3-10 MeV



High Energy Protons ~ 1 GeV



Protons Image Blurring Due to Multiple Coulomb Scattering

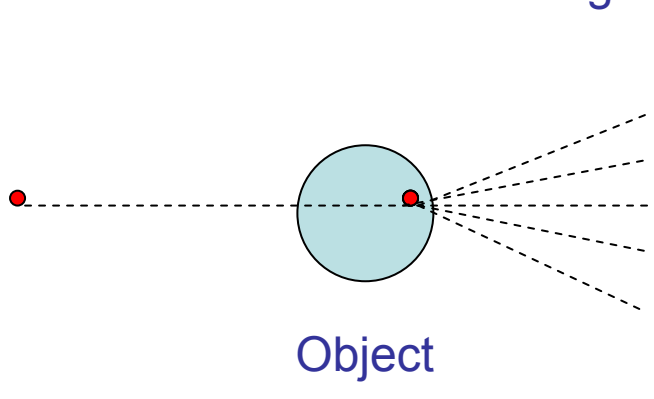
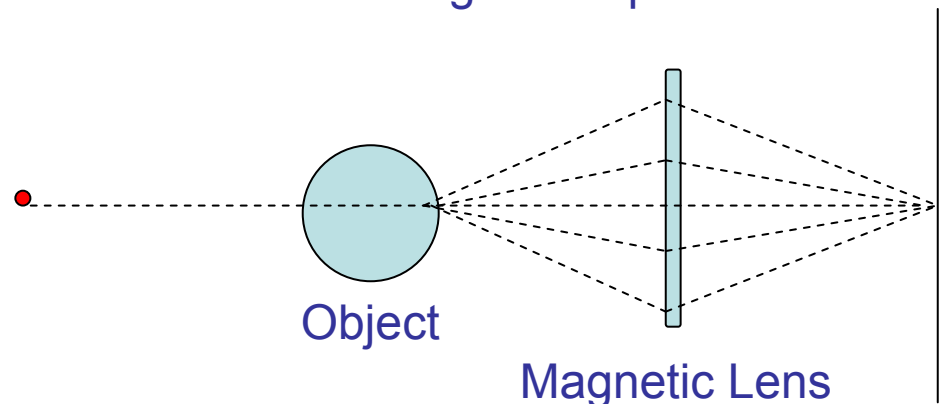


Image Blurring compensation with Magnetic Optics



A. M. Koehler, *et al.* *Science* **160**, 303 (1968)

J. A. Cookson *Naturwissenschaften* **61**, 184—191 (1974)

C.L. Morris, J.D. Zumbro, Overview of proton radiography—concepts and techniques, Technical Report LA-UR-97-4172, Los Alamos National Laboratory, 1997.

# Advantages of Proton Radiography

as compared with X-rays

- magnetic lenses for correcting imaging aberrations
- high resolution and dynamic range to both density and material composition
- better signal-to-noise ratio and detection efficiency
- higher penetrating depth (targets with high areal density)
- multi-framing capability

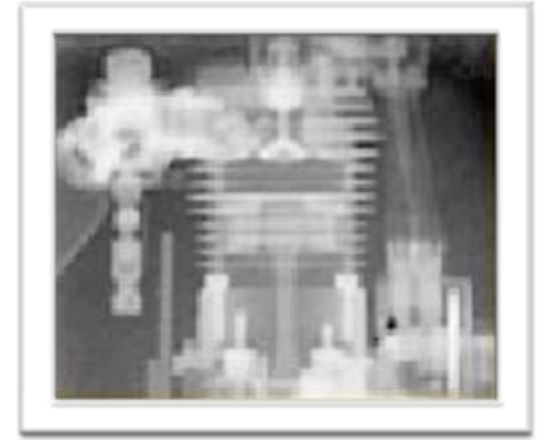
photo



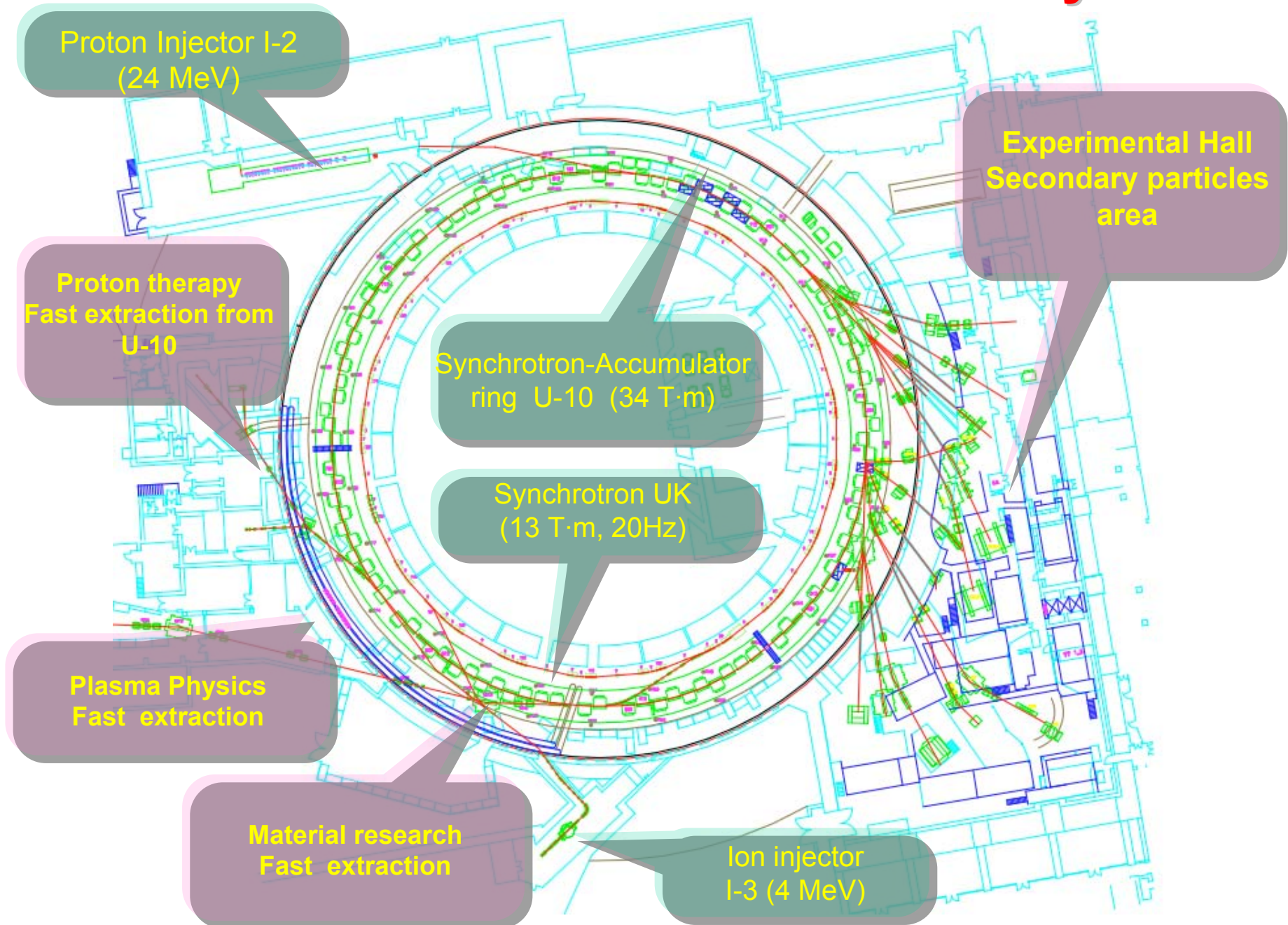
100 keV X-rays



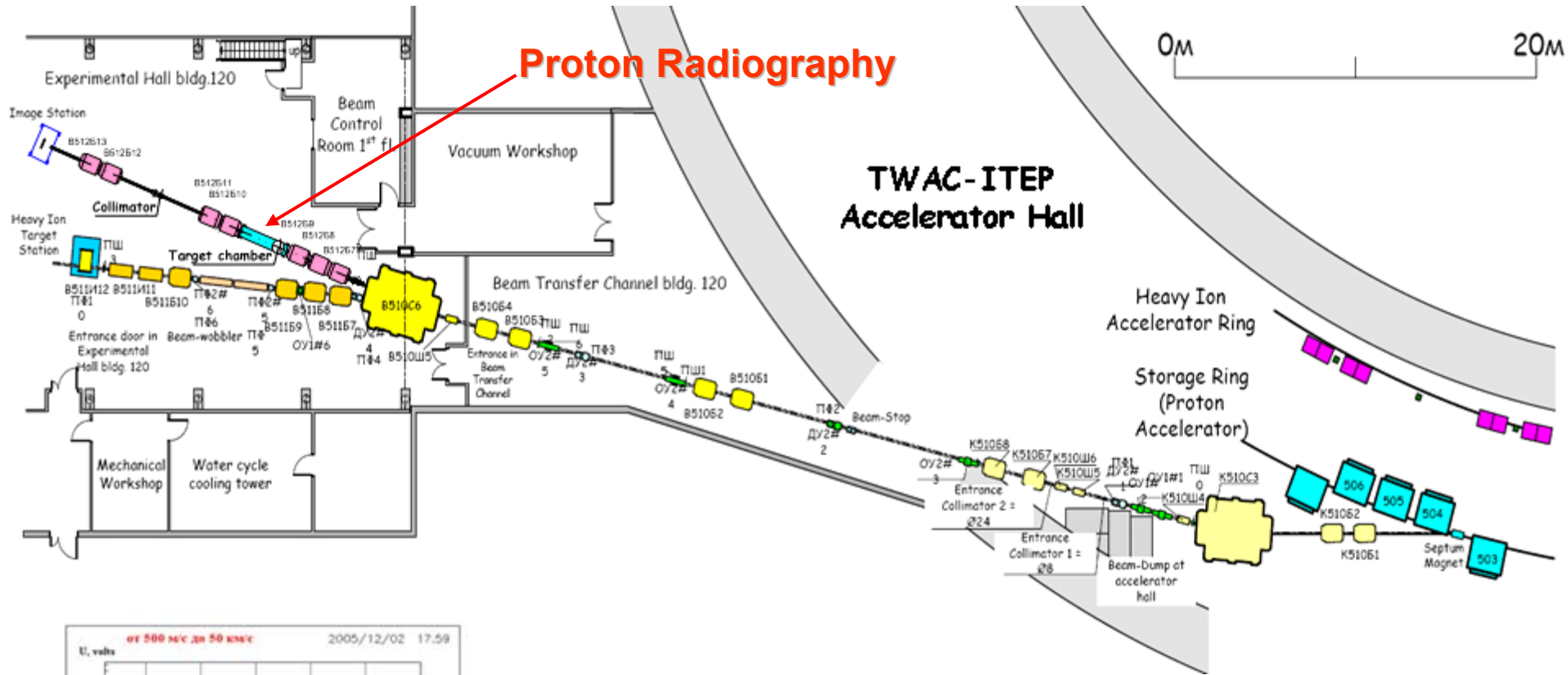
800 MeV protons



# ITEP-TWAC Accelerator Facility



# Proton Radiography Facility at ITEP-TWAC Accelerator

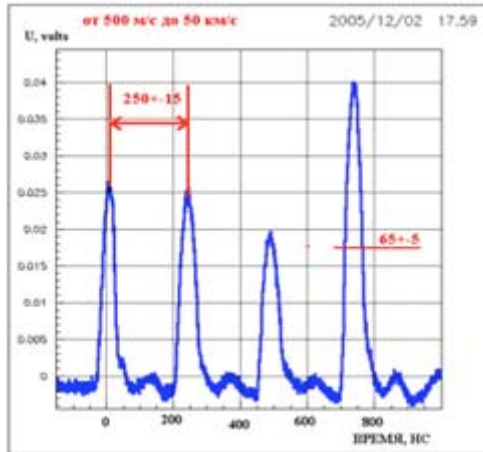


Proton Radiography

TWAC-ITEP  
Accelerator Hall

Heavy Ion  
Accelerator Ring

Storage Ring  
(Proton  
Accelerator)



## 800 MeV Proton Beam Line

Beam structure – 3-4 bunches (See image on the left)

Duration of single bunch (FWHM): **70 ns**

Interval between bunches: **250 ns**

Beam intensity: up to  **$10^{11}$**  protons

# Proton Radiography Facility at ITEP-TWAC Accelerator



## ITEP Proton Microscope

4 permanent quadrupole magnets  
Magnification  $X = 3.92$   
Field of view  $< 19 \text{ mm}$   
Spatial resolution on sharp contrast object:  $\sigma = 50 \mu\text{m}$   
Density resolution  $\sim 6\%$

## Explosion Confinement Chamber

Volume – 50 liters  
HE mass (TNT) – up to **70 g**  
Pumped down to  $10^{-3}$  Torr  
Active ventilation system  
Optical diagnostics - VISAR  
Target angular positioning ( $\pm 10^\circ$ )  
Cryogenic target system

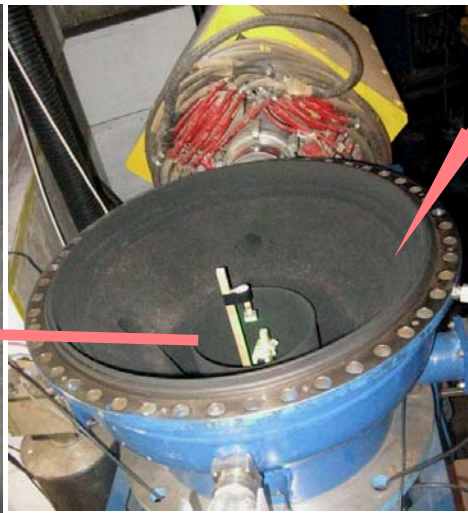
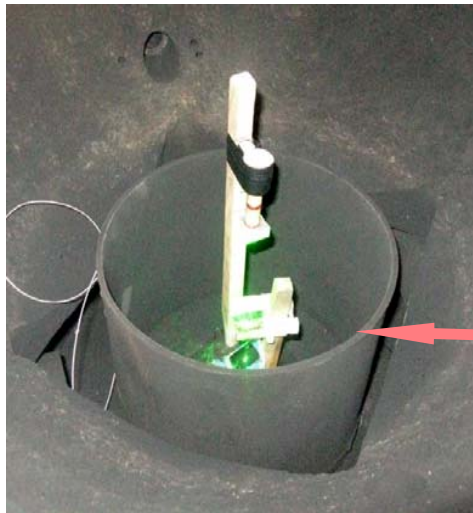
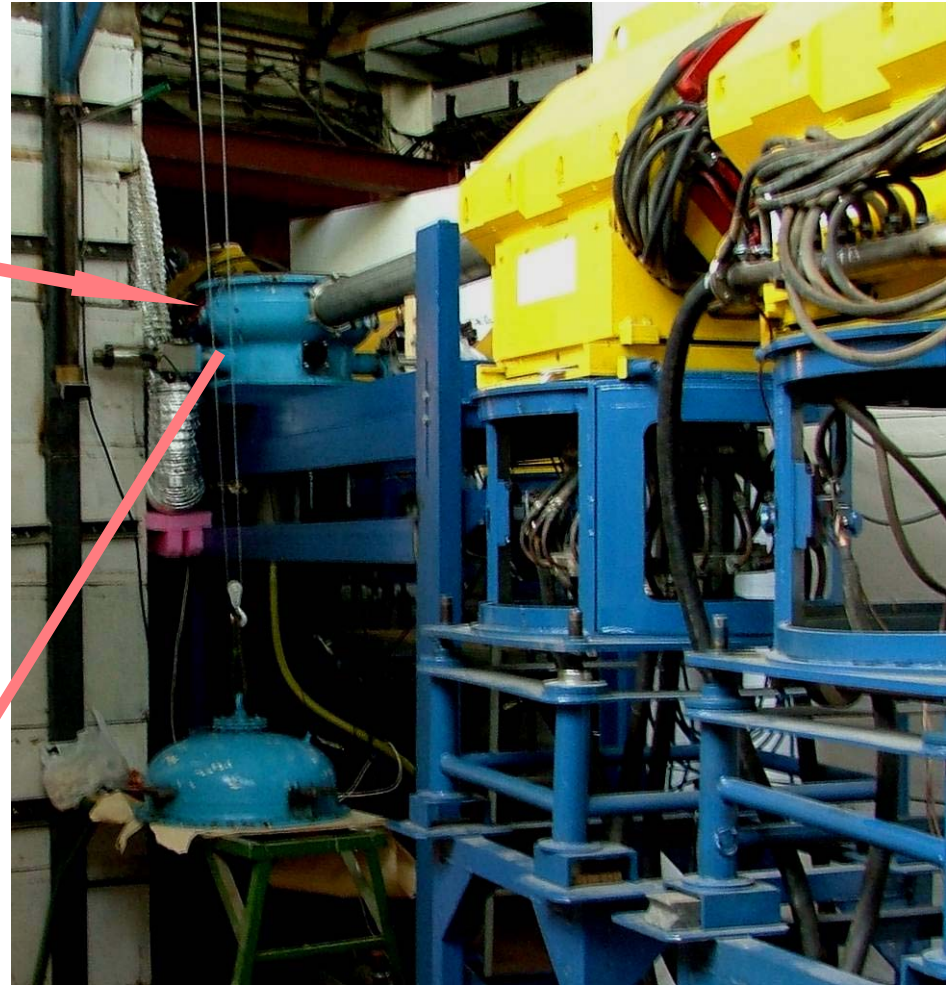


## Image Registration System

Optical converter: LSO scintillator (40 ns),  $\varnothing 78 \text{ mm}$   
3-6 14 bit CCD cameras, fast shutter (100 ns),  
matched to beam bunch;  
Temporal resolution = Bunch duration = **70 ns**

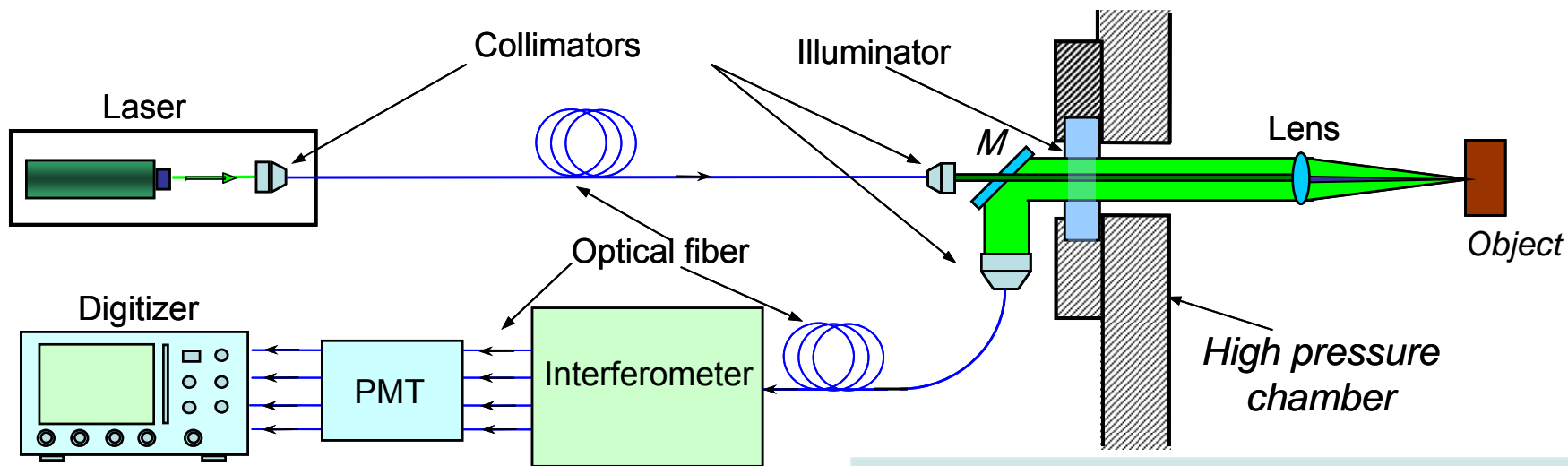


# Experimental Area





# Push-Pull VISAR for Proton Radiography at ITEP



**Laser**  
 Wavelength 532 nm  
 Line width <5 MHz  
 Power 50 mW

$$I_1 = I_0 \sin 2\pi N(t) + A(t)$$

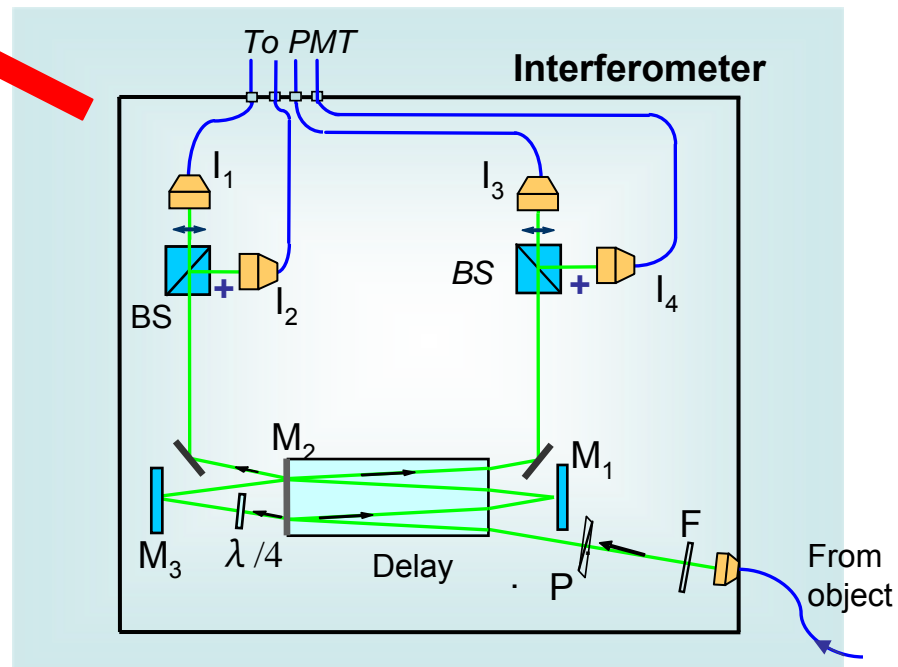
$$I_2 = I_0 \cos 2\pi N(t) + A(t)$$

$$I_3 = -I_0 \sin 2\pi N(t) + A(t)$$

$$I_4 = -I_0 \cos 2\pi N(t) + A(t)$$

$$V(t) = \frac{c\lambda}{8\pi d(n-1/n)(1+\delta)} \arctg \frac{I_1 - I_3}{I_2 - I_4}$$

by A. Kuznetsov, K. Gubsky

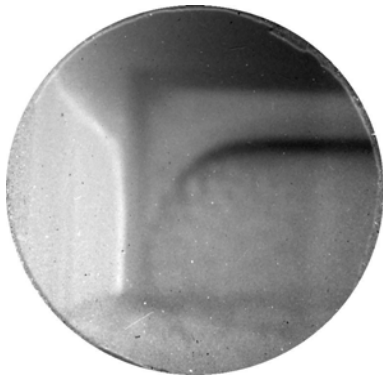


# Proton Radiography for High Energy Density Physics

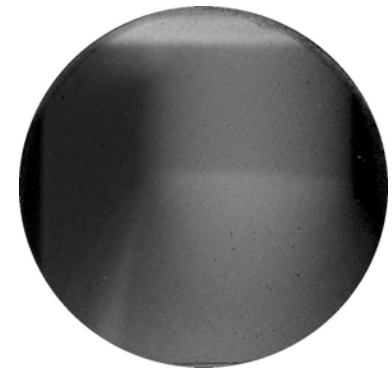
## HEDP

Research areas that can be addressed by Proton Radiography

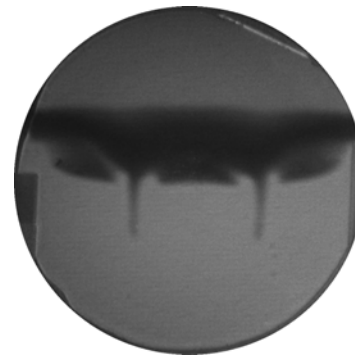
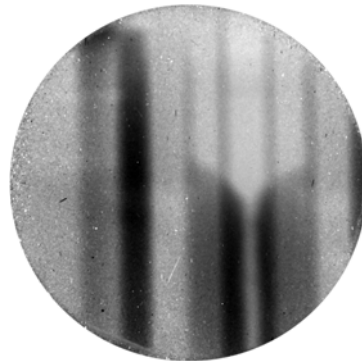
**EoS and Phase Transitions**  
in materials in extreme conditions



**Hydrodynamics of HED Flows**  
Shock and Detonation Waves,  
Hydrodynamic Instabilities



**Material Strength and Damage**  
Dynamic Fracture of Materials

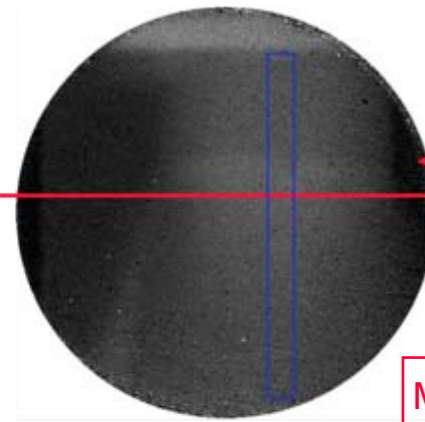
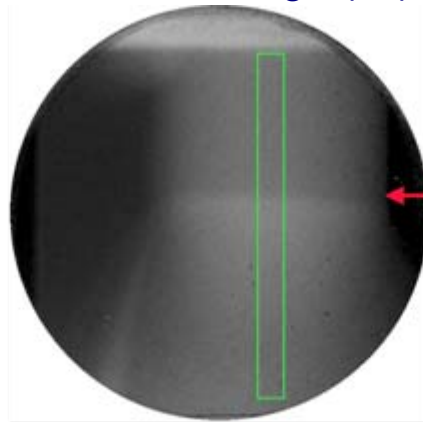
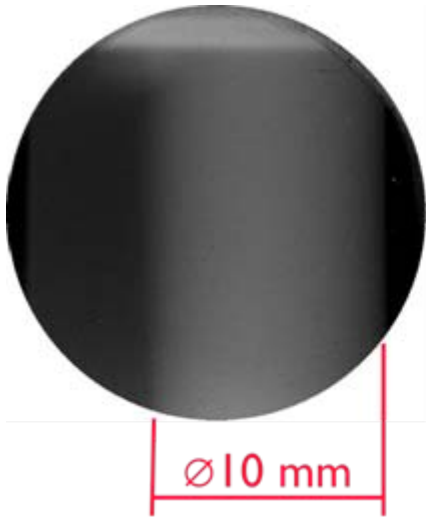


# Detonation of Pressed TNT

Static image

Bunch 2 image ( $T_2$ )

Bunch 3 image ( $T_3$ )



$\Delta T = T_3 - T_2 = 250 \text{ ns}$   
 $\delta T = 70 \text{ ns}$   
 $\Delta X = 1.72 \pm 0.05 \text{ mm}$   
 $D = \Delta X / \Delta T = 6.9 \pm 0.2 \text{ km/s}$   
 Front curvature radius:  
 $R = 58 \pm 7 \text{ mm}$

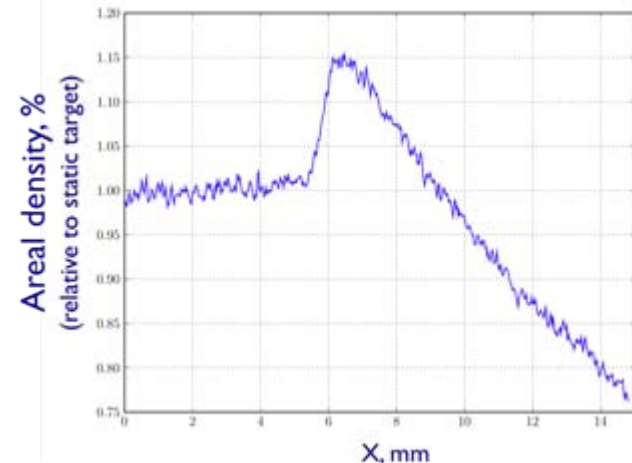
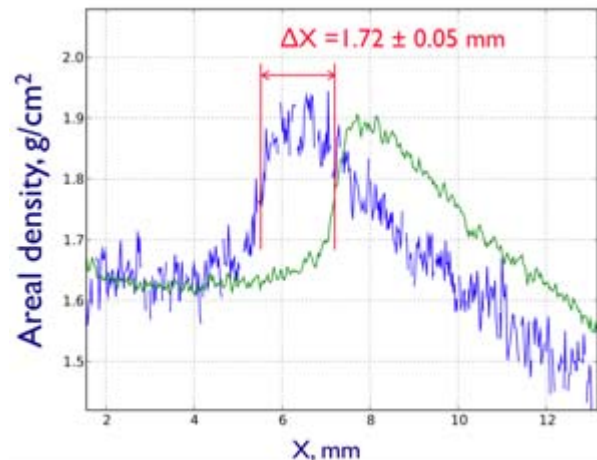
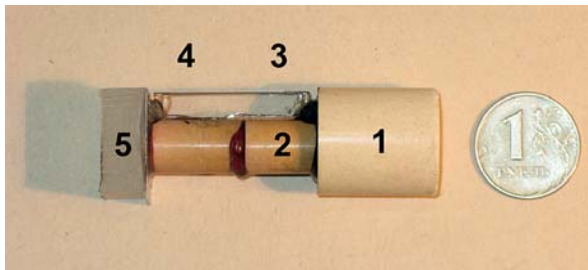
Motion blur  $\delta X = D \delta T = 0.48 \text{ mm!}$

Total HE weight 25g  
 Initial density 1.32 - 1.65 g/cc  
 Charge diameter 10; 15; 20 mm  
 Charge length 30-56 mm

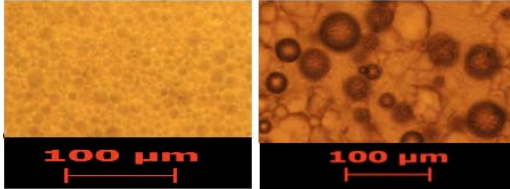
Above: proton radiography images of static (left) and dynamic detonating 10 mm TNT charge with initial density of 1.63 g/cc.

Below, left: photo of experimental target. 1 – initiating HE charge, 2 – target charge, 3 – reference plastic plate, 4,5 – VISAR reflective Al surface and diagnostic window.

Below: absolute (center) and relative (left) areal density profiles for the TNT charge.



# Detonation of Emulsion Explosive

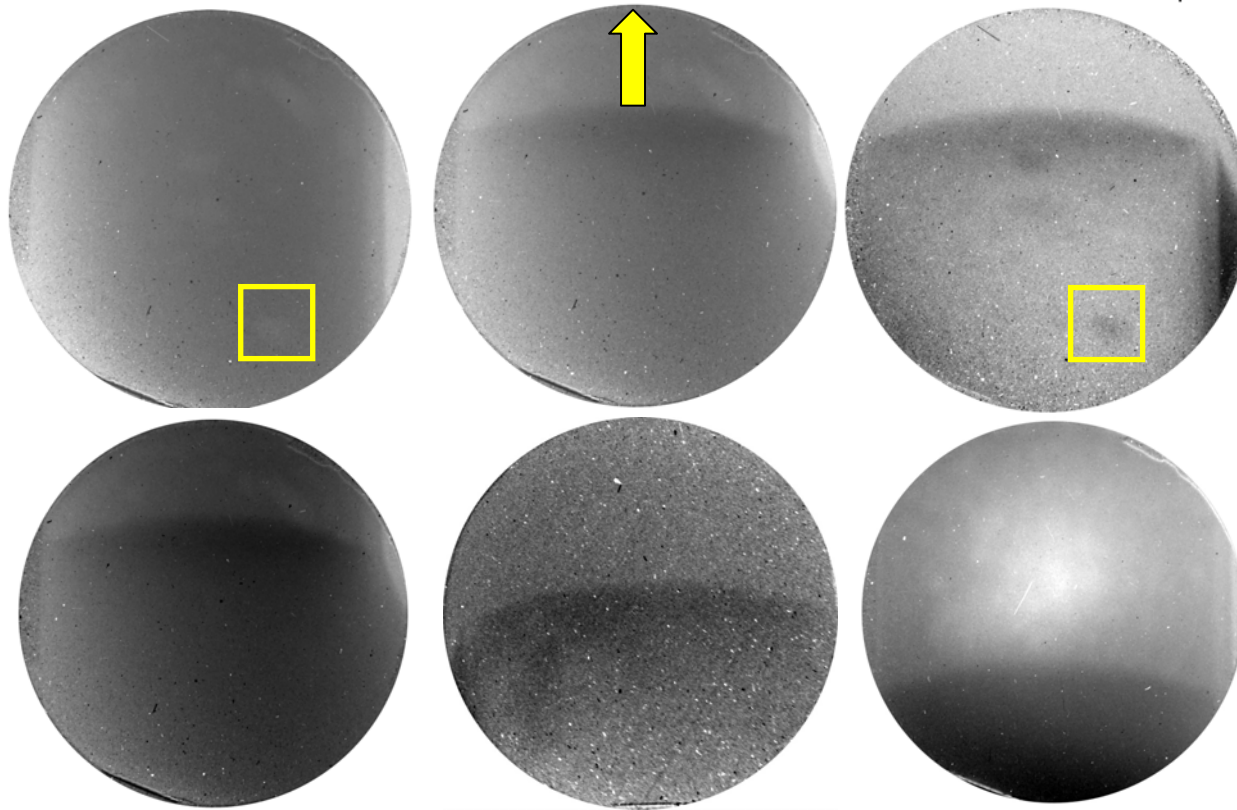
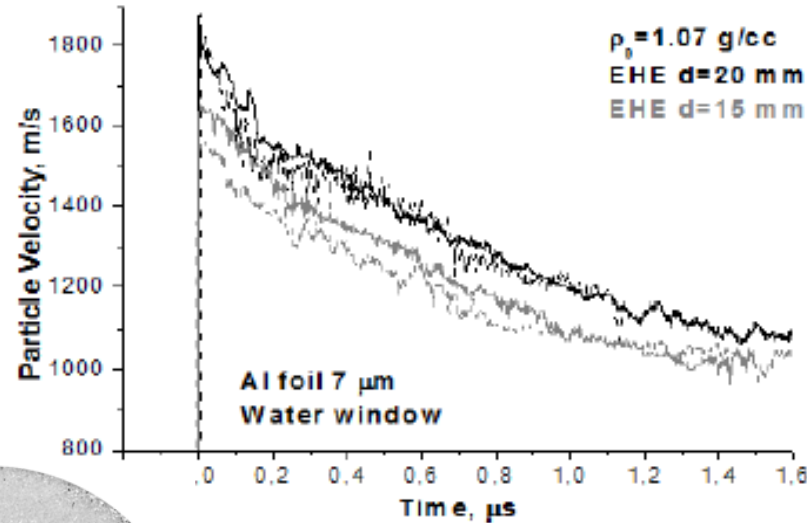


## Emulsion Explosive

92-95% - oxidizer (ammonium nitrate)  
 8-5% - fuel (mineral oil)  
 + 3 wt.% - hollow glass microballoons  
 Density 1.07 g/cc  
 Charge diameter 15; 20; 36 mm  
 Charge length 60-150 mm

## Experimental target

1 – initiating HE charge, 2 – plastic flange  
 3 – polyethylene tube with studied emulsion explosive, 4,5 – VISAR reflective 7 μm Al surface and plastic diagnostic window.

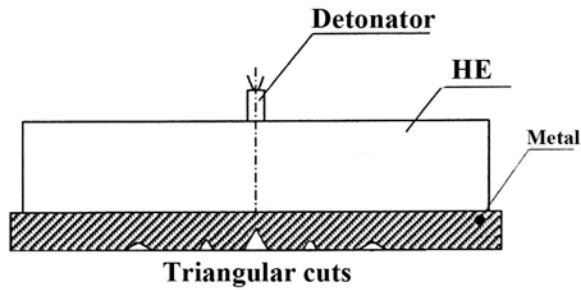


Static, dynamic and relative proton radiography images of 20 mm emulsion explosive charge. Yellow arrow points to the direction of wave propagation. Yellow frame points to one of the inhomogeneities of the initial charge.

Detonation velocity  $D = 4.6 \pm 0.2$  km/s

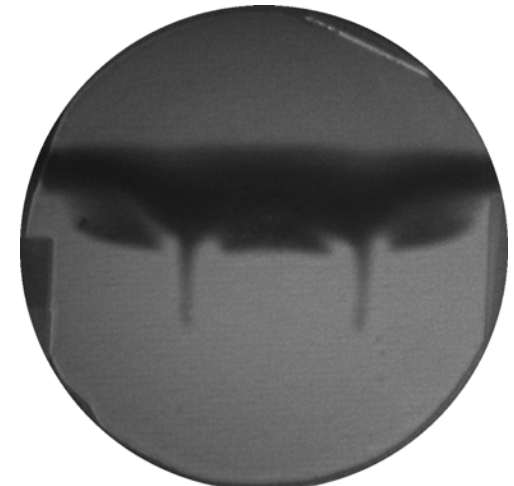
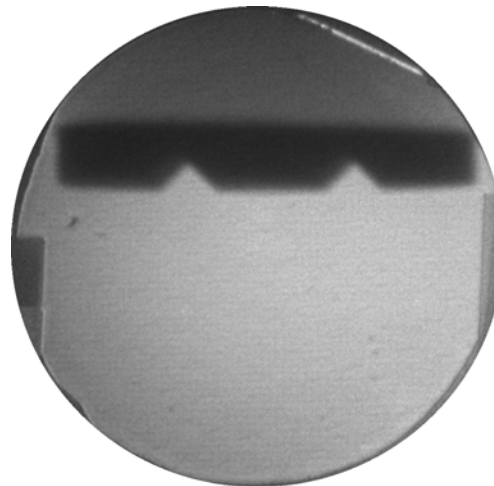
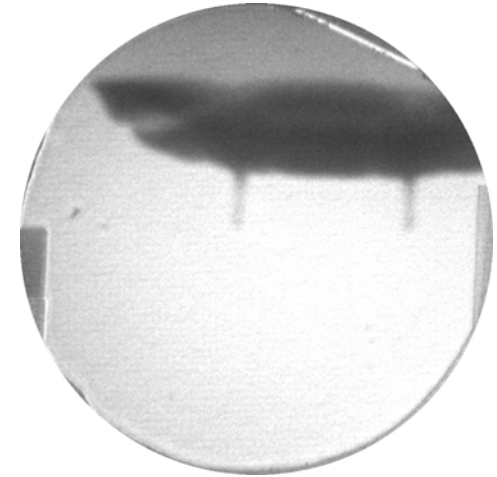
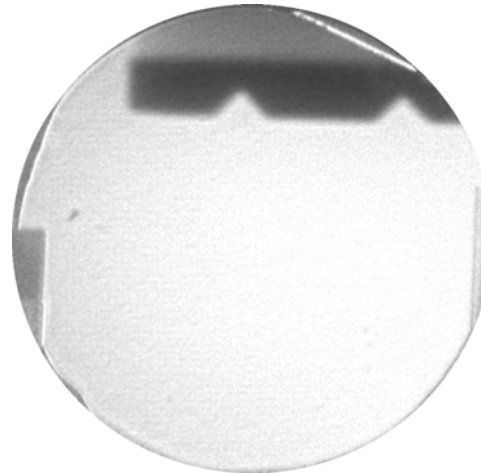
Dynamic proton radiography images for different 15 mm emulsion explosive charges: left – steady-state detonation ( $D=4.4$  km/s), center – non-steady detonation-like wave ( $D=4.4$  km/s), right – fading shock wave ( $D \sim 4.0$  km/s)

# Dynamic Fracture and Surface Ejecta Formation in Metals under Shock Loading



Proton radiography images of static targets

Proton radiography images of dynamic shots at 2.5  $\mu$ s after shocking the free surface of a target



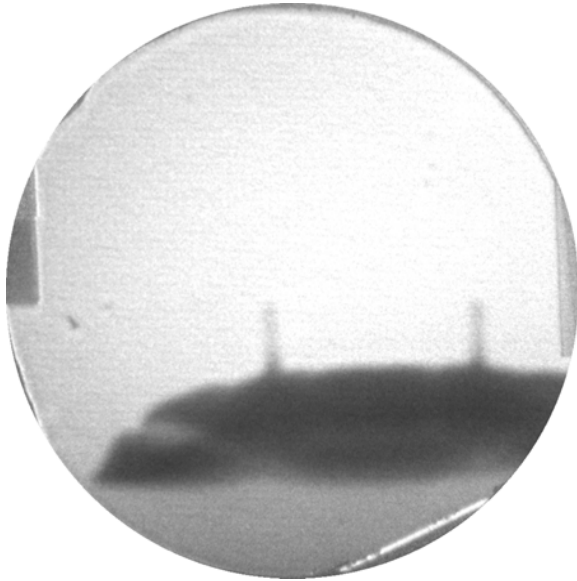
## Steel target

Diameter – 15 mm  
Thickness – 2 mm  
Depth of cuts – 1 mm

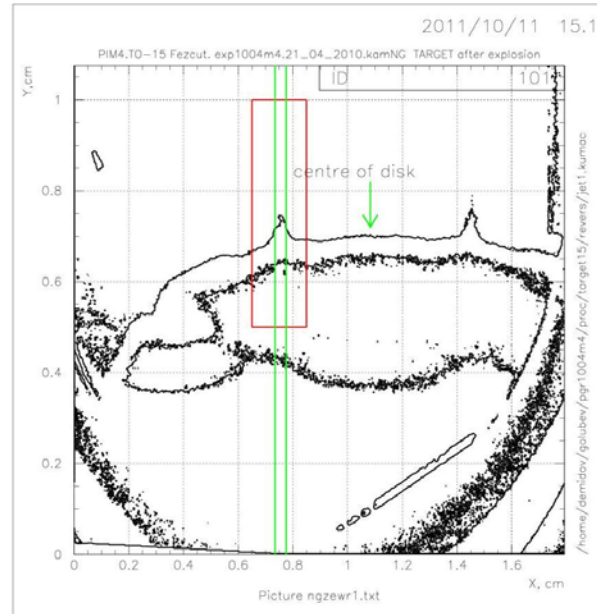
## Copper target

Similar to steel one

# Dynamic Fracture and Surface Ejecta Formation in Metals under Shock Loading

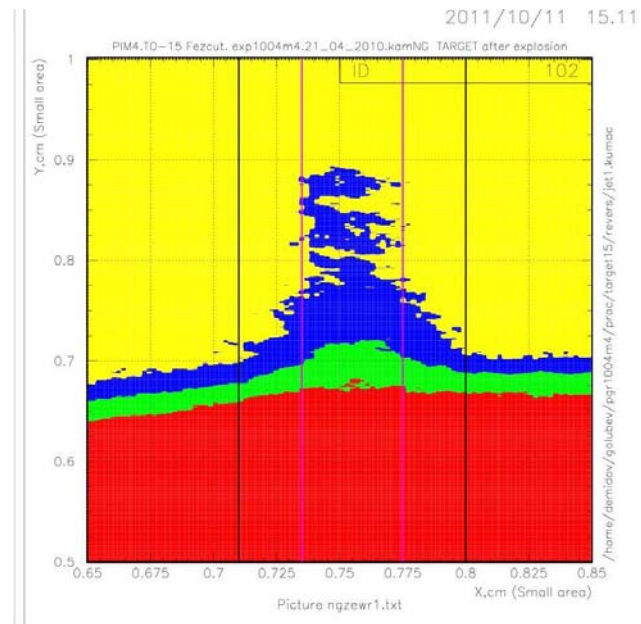


Dynamic proton radiography image shot at  $2.5 \mu\text{s}$  after shocking the free surface of the steel target



Linear density map reconstructed from radiographic image

**Velocity of jet tip:  
2.8 km/s**



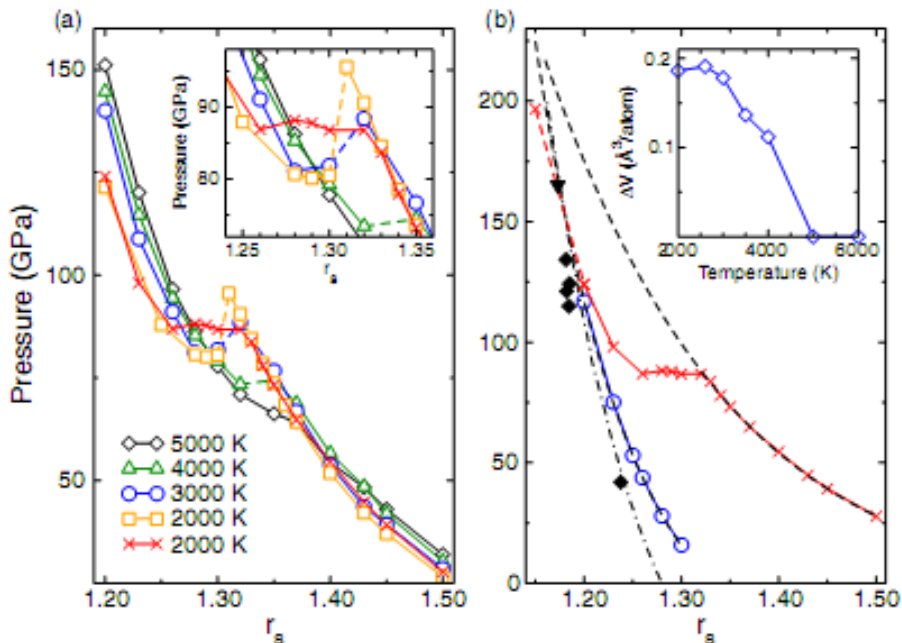
Close-up of the area inside the red frame on the left image

**Mean volume density of  
jet material: 0.08 g/cc**

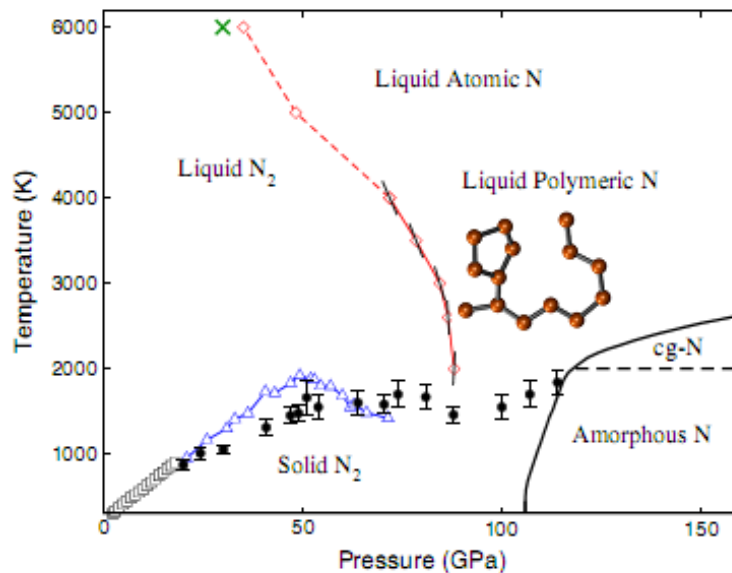
# Development of Compact Explosive Generators

for Studies of First-Order Liquid-Liquid Phase Transition in Compressed Nitrogen

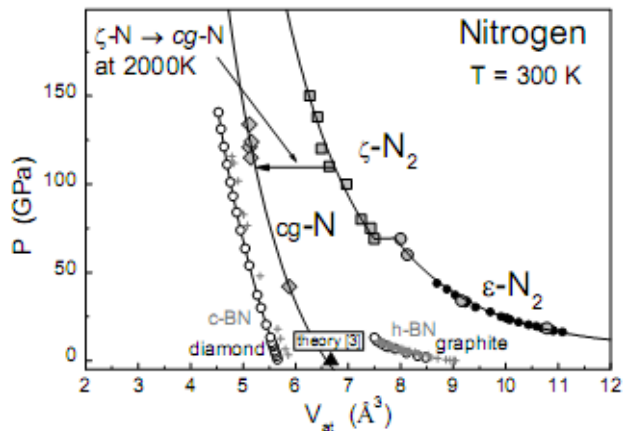
B. Boates, S. Bonev. PRL 102, 015701 (2009)



QMC calculations of nitrogen isotherms:  
X – liquid phase. O – solid phase



Proposed nitrogen phase diagram in P-T coordinates. Region of possible existence of liquid polymeric phase is shown.



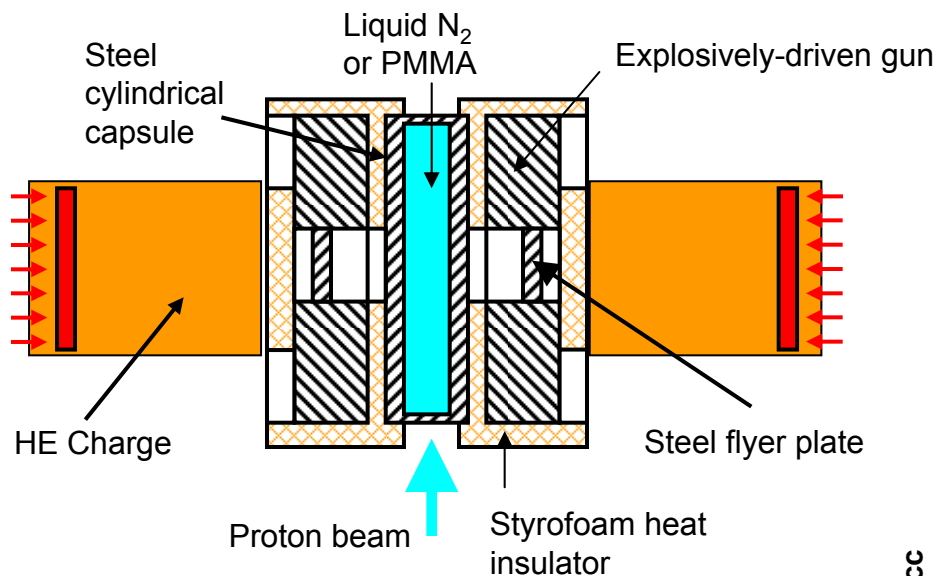
Experiment: nitrogen compression and heating in DAC

Structural transformation of molecular nitrogen to a single-bonded atomic state at high pressures. M. Eremets, A. Gavriluk et al. J Chem Phys. 2004 121(22):11296

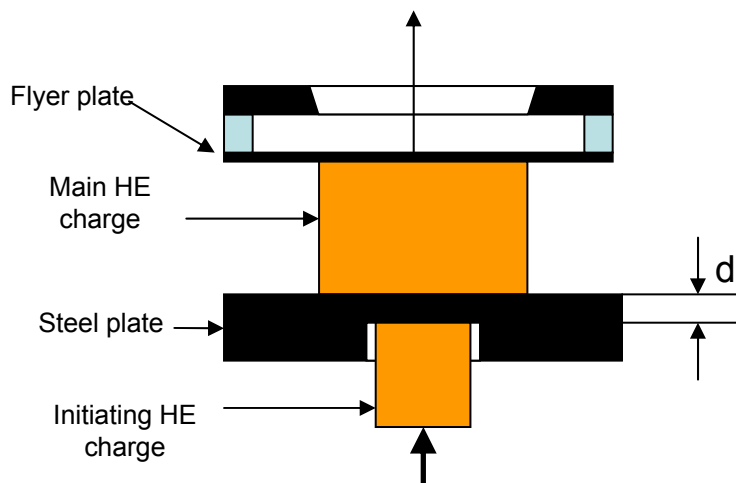
Transition of nitrogen to liquid polymeric phase is expected at compression of 75-100 GPa, temperature 2000 K and density jump of about 20-24%. This jump is very large for structural phase transition, which makes it a good object for proton radiography studies.

# Development of Compact Explosive Generators

for Studies of First-Order Liquid-Liquid Phase Transition in Compressed Nitrogen

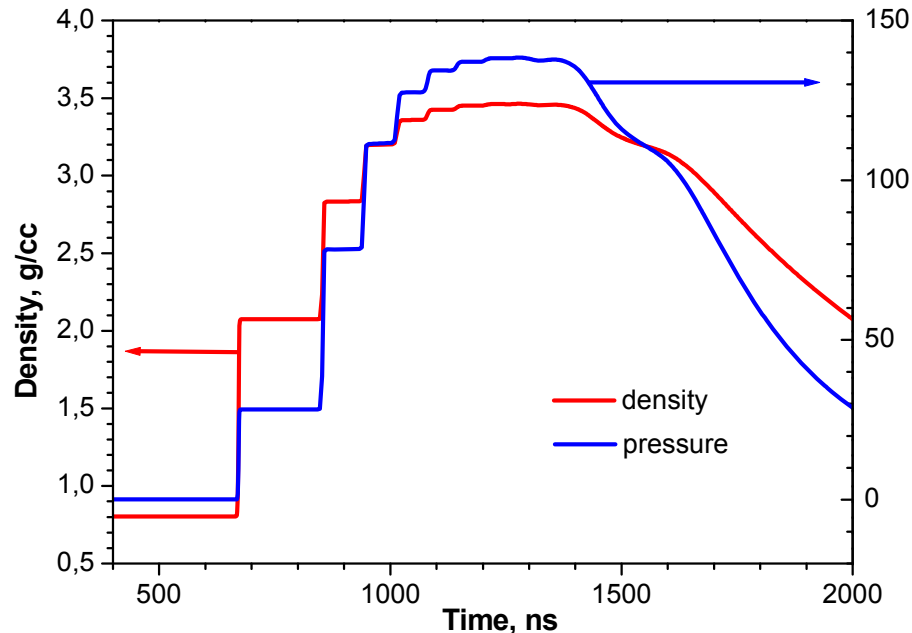


Scheme of experiment



Scheme of compact explosively-driven gun

**Problem:** limited HE capacity of existing explosive confinement chamber (70 g of TNT), which requires the development of new compact explosive generators.

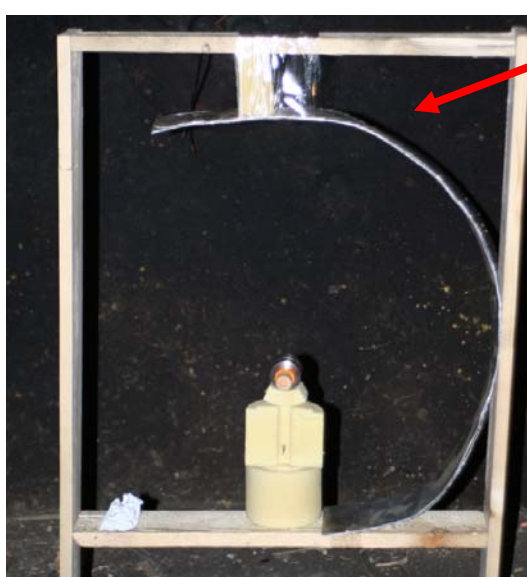
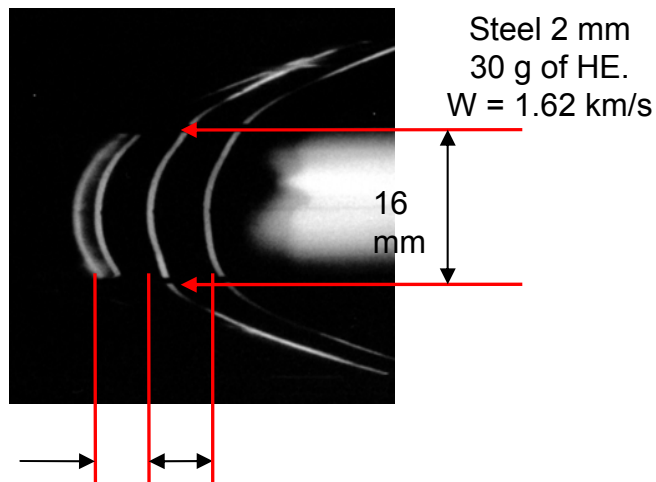


Pressure and density calculations for liquid N<sub>2</sub>; flyer plate velocity - 2.2 km/s



# Development of Compact Explosive Generators

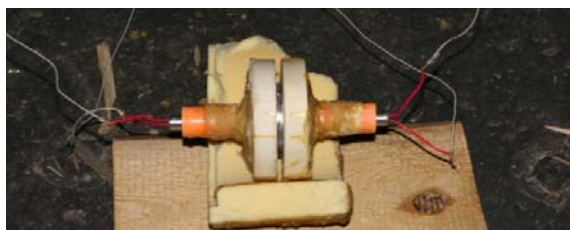
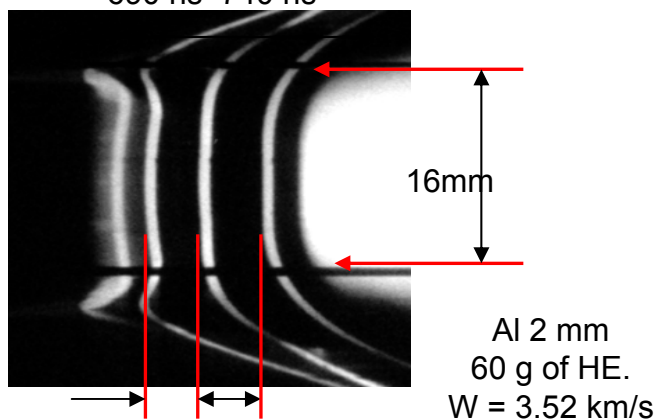
for Studies of First-Order Liquid-Liquid Phase Transition in Compressed Nitrogen



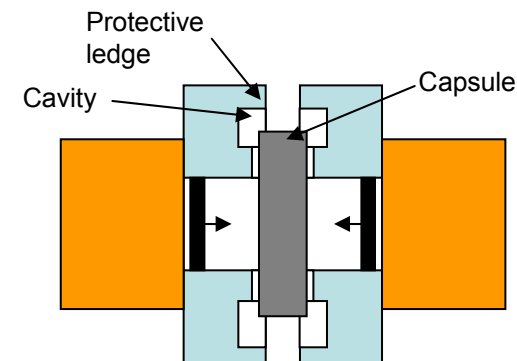
Al 0.75 mm sheet



Penetration of fragments through sheet



Cavity for capturing the fragments is required within the developed "gun"



Scheme of improved compact explosive generator

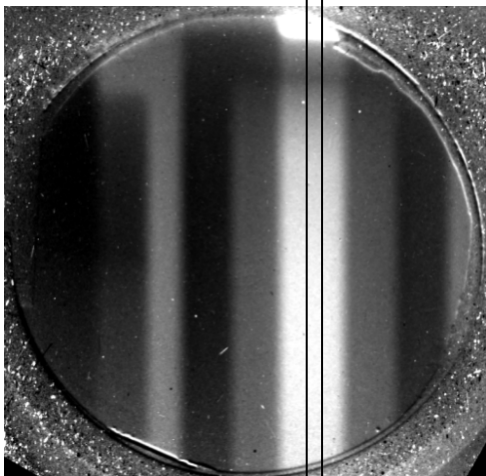
665 ns 710 ns  
time

Flyer plate shape testing  
and mitigation development

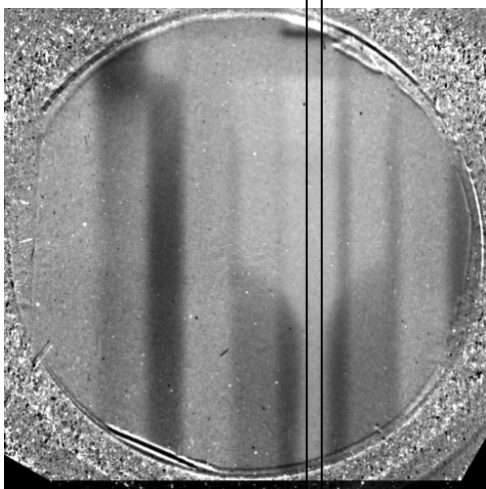
# Development of Compact Explosive Generators

## for Studies of First-Order Liquid-Liquid Phase Transition in Compressed Nitrogen

Static image

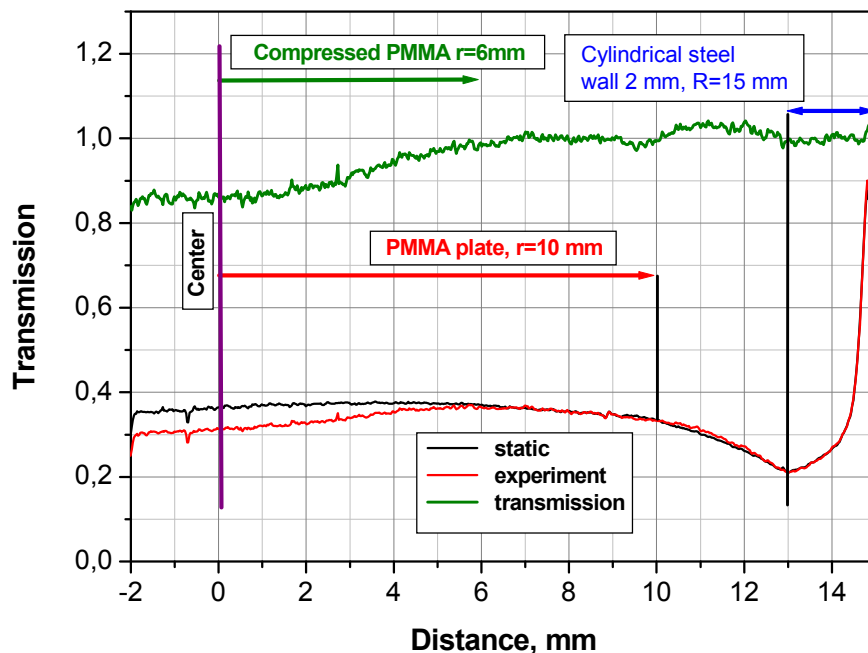
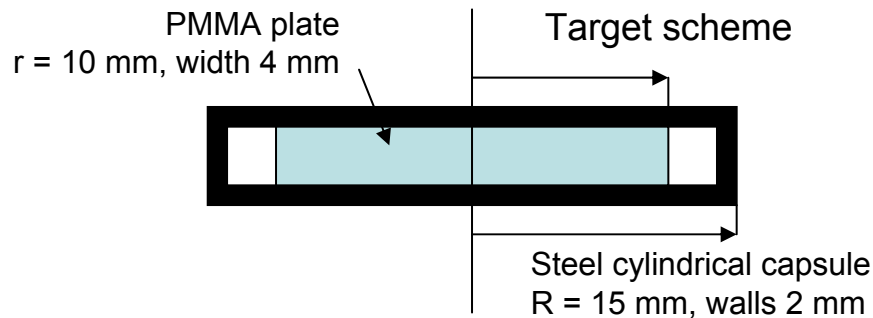


Cross-section where the density profile is taken



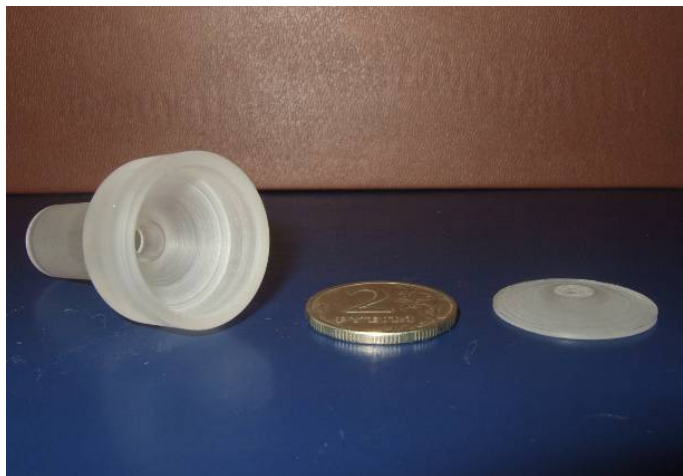
Moment of compression

Proton radiography registration of bilateral compression of test PMMA target

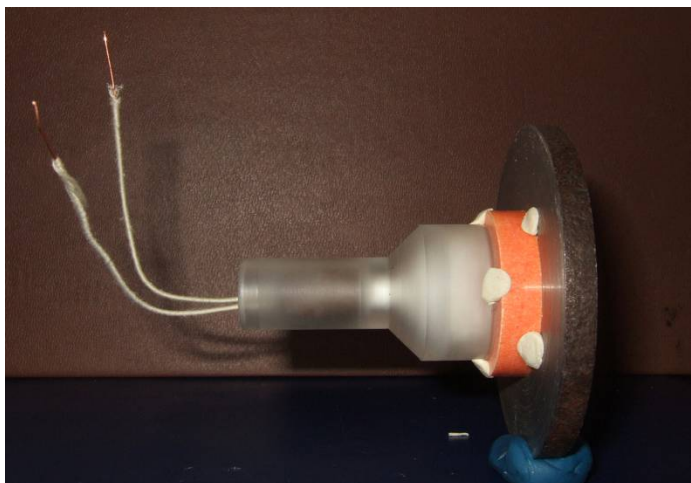


Transmission profiles (relative to the "white field" intensity) for static and 1<sup>st</sup> dynamic proton radiography shots. Relative transmission profile (divided by static profile) for compressed PMMA is also presented.

# Development of Compact Explosive Generators



Plexiglass components of compact explosive generator



Experimental assembly for accelerating flyer plate with compact explosive generator

Total amount of explosive

< 15 g of TNT

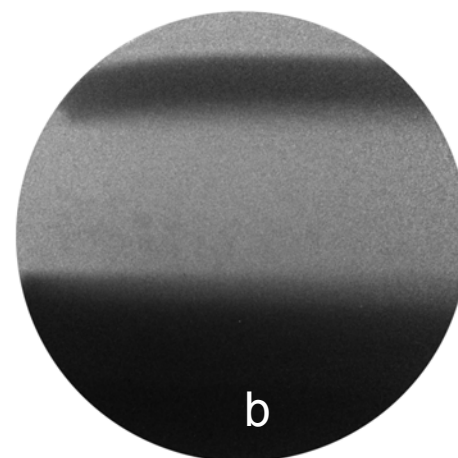
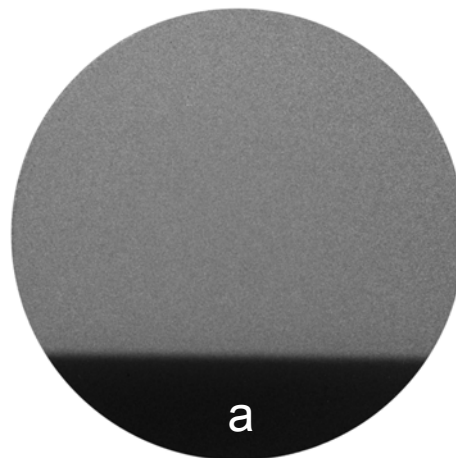
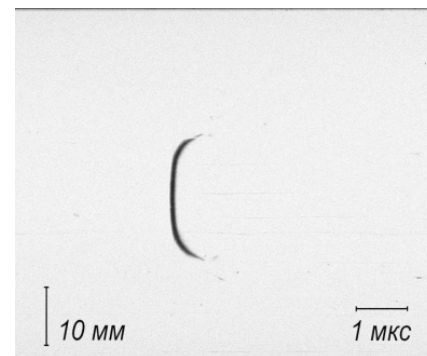
Flyer plate

∅20, 1-2 mm thick

Flyer plate material

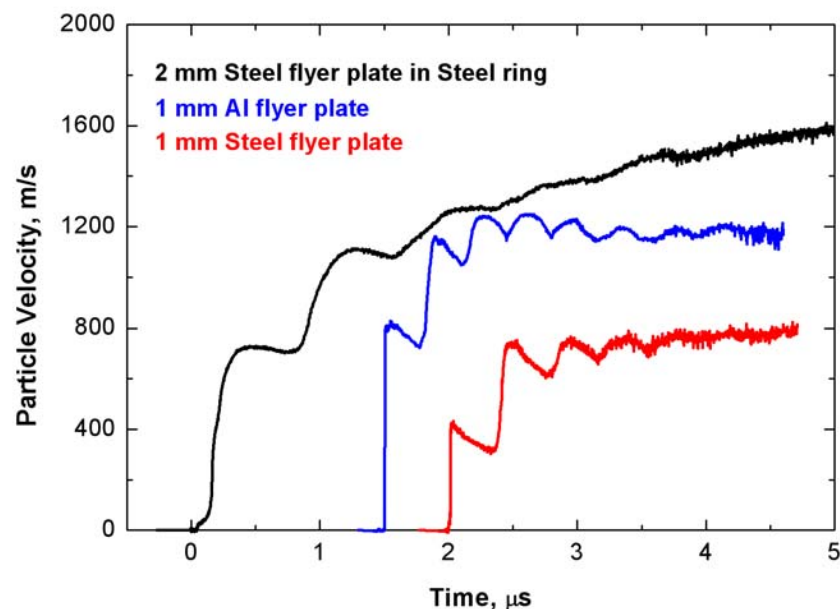
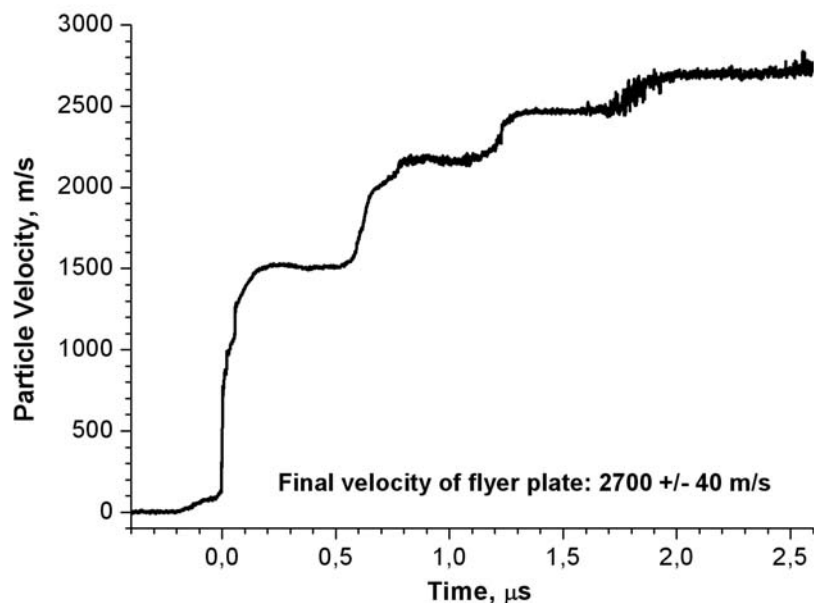
Al, Steel

To the right: high-speed photoregistrator image of shock wave from 1 mm Al flyer plate accelerated with compact explosive generator



Proton radiography images of 2 mm thick ∅20 Al flyer plate acceleration: a) static image; b) dynamic shot at 4.75 μs after start

# Development of Compact Explosive Generators

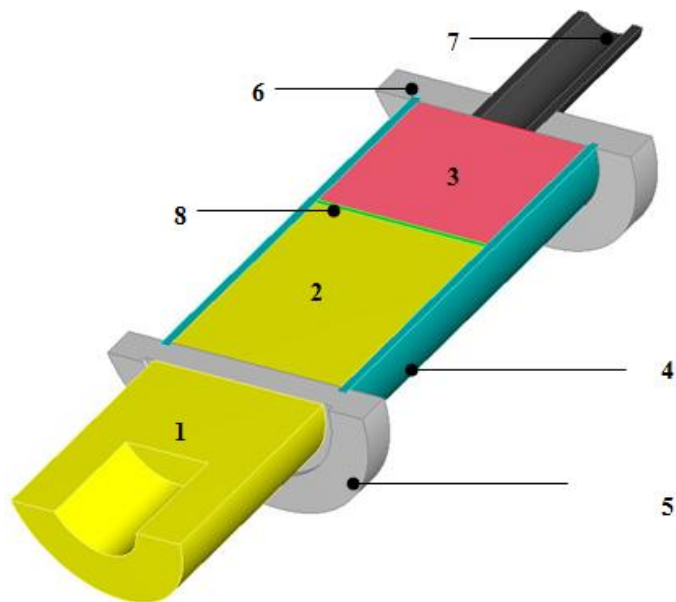


VISAR flyer plate free surface profiles: *left* – for 2 mm Al flyer plate, *right* – for 1 mm Al and 1 & 2 mm Steel flyer plates

Flyer plate	Velocity after full acceleration, km/s	Base of flight, mm	Diameter of plane region, mm
2 mm Al in Steel ring	<b>2.8</b>	10	13
2 mm Steel in Steel ring	<b>1.6</b>	6	
1 mm Al	<b>1.2</b>	3	13
1 mm Steel	<b>0.8</b>	2	

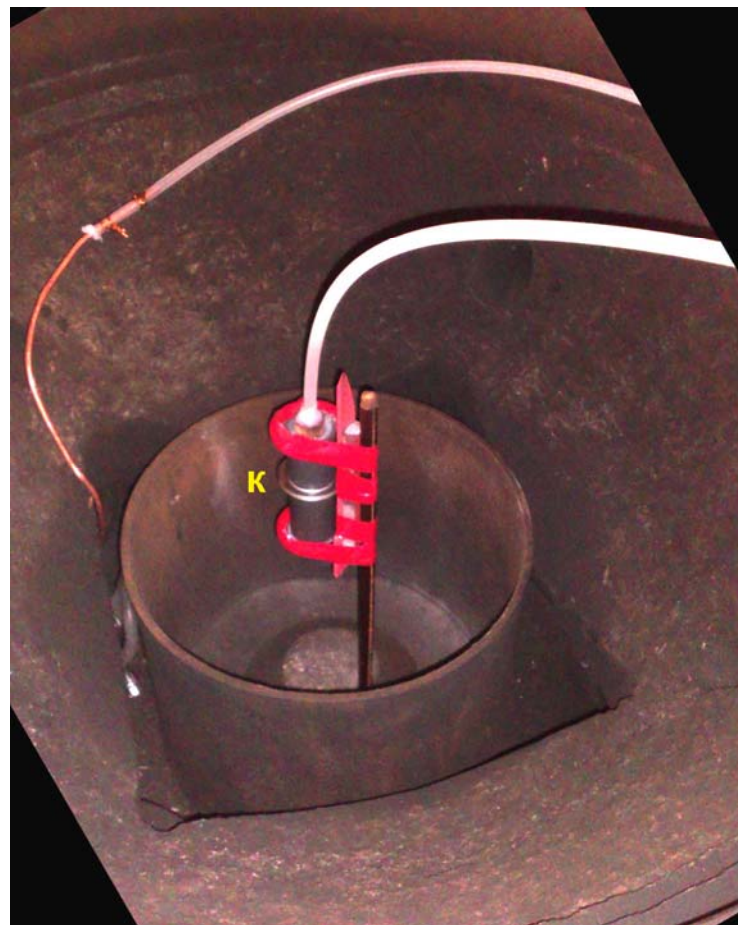
# Shock Compression of Noble Gases

## Target scheme



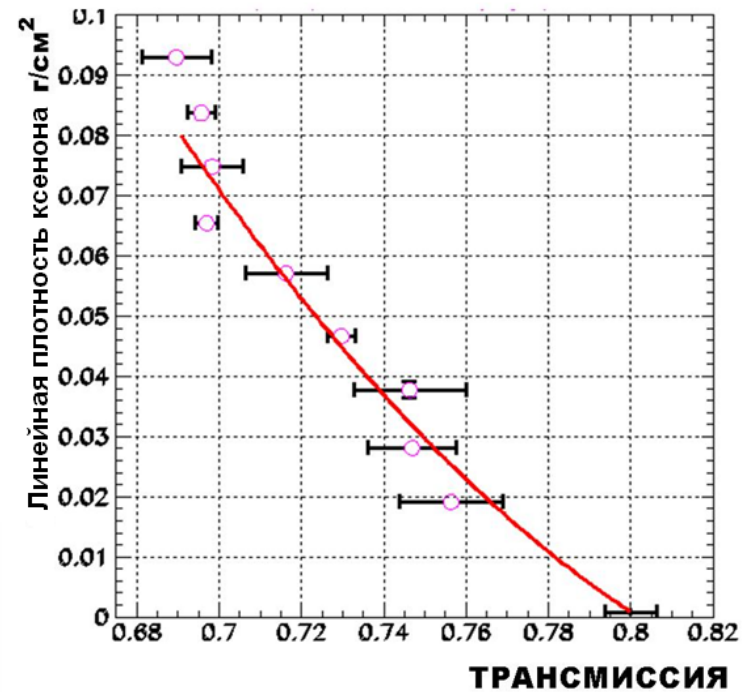
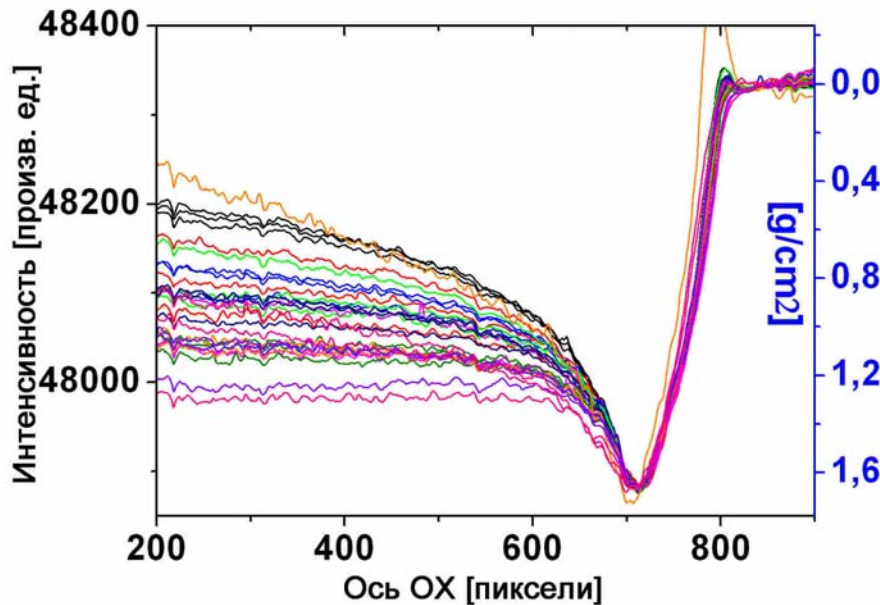
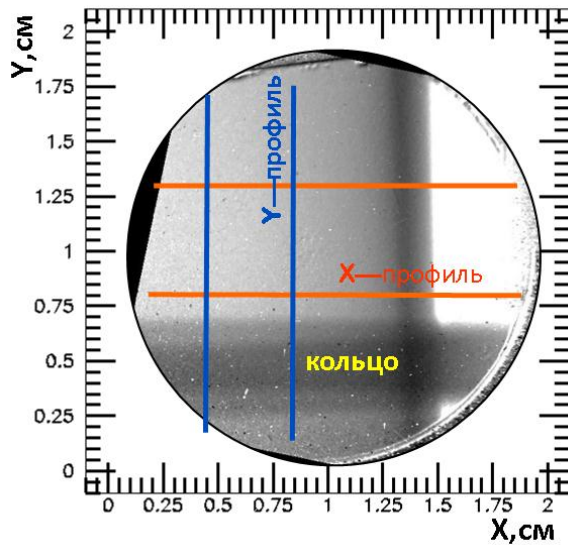
- 1,2 – HE tablets,
- 3 – investigated noble gas,
- 4 – generator canal,
- 5, 6 – leak-proof flanges,
- 7 – tube for gas system

Studied gases: Ar, Xe  
Initial pressure:  $\sim 1-5$  Bar  
Shock wave velocities:  $\sim 4-6$  km/s



# Shock Compression of Noble Gases

Calibration of Density vs Transmission for Static Targets with Xe for Pressures 0-10 Bar



Above, left: static proton radiography image of gas container with Xe

Left: normalized light intensity profiles for different initial densities from 0 to 10 Bars, taken between horizontal red lines on static image

Above: calibration dependence of linear density vs proton beam transmission, calculated from the image on the left

# Shock Compression of Noble Gases

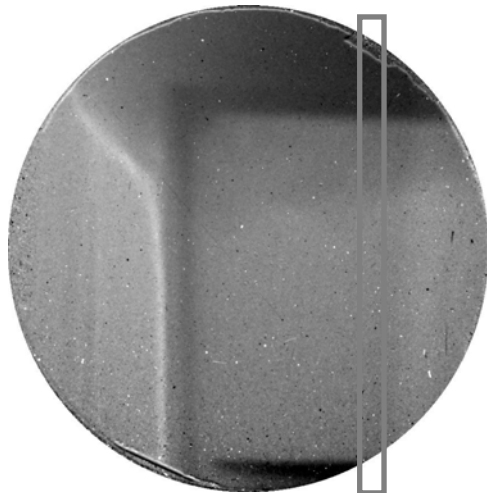
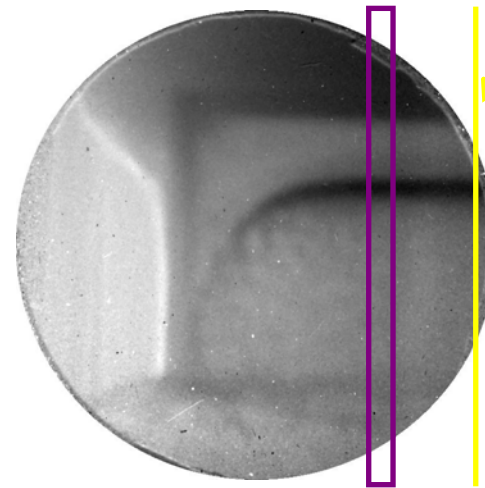
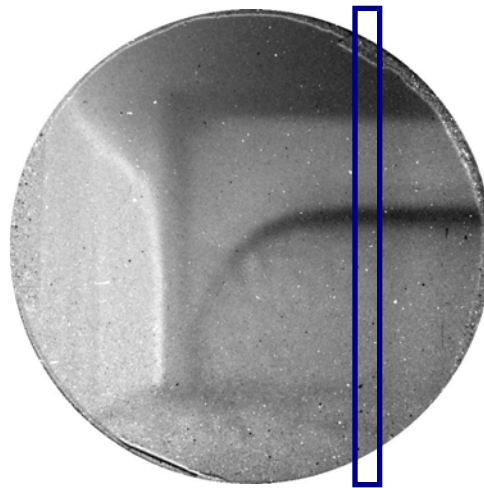
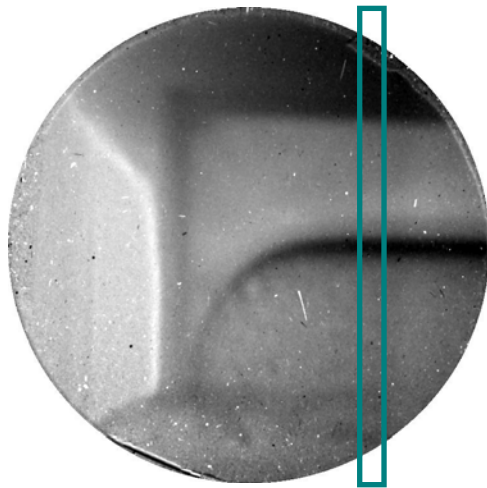
Xenon  $P_0 = 2.5$  Bar

Camera 1  
Proton bunch 1 ( $t_1$ )

Camera 2  
Proton bunch 2 ( $t_2$ )

Camera 3  
Proton bunch 3 ( $t_3$ )

Target axis



$$\Delta t = t_2 - t_1 = t_3 - t_2 = 250 \text{ ns}$$
$$\delta t(\text{FWHM}) = 70 \text{ ns}$$

1 mm

4.19 mm

Gas cell thickness - 20.34 mm

Gas pressure - 2.5 Bar

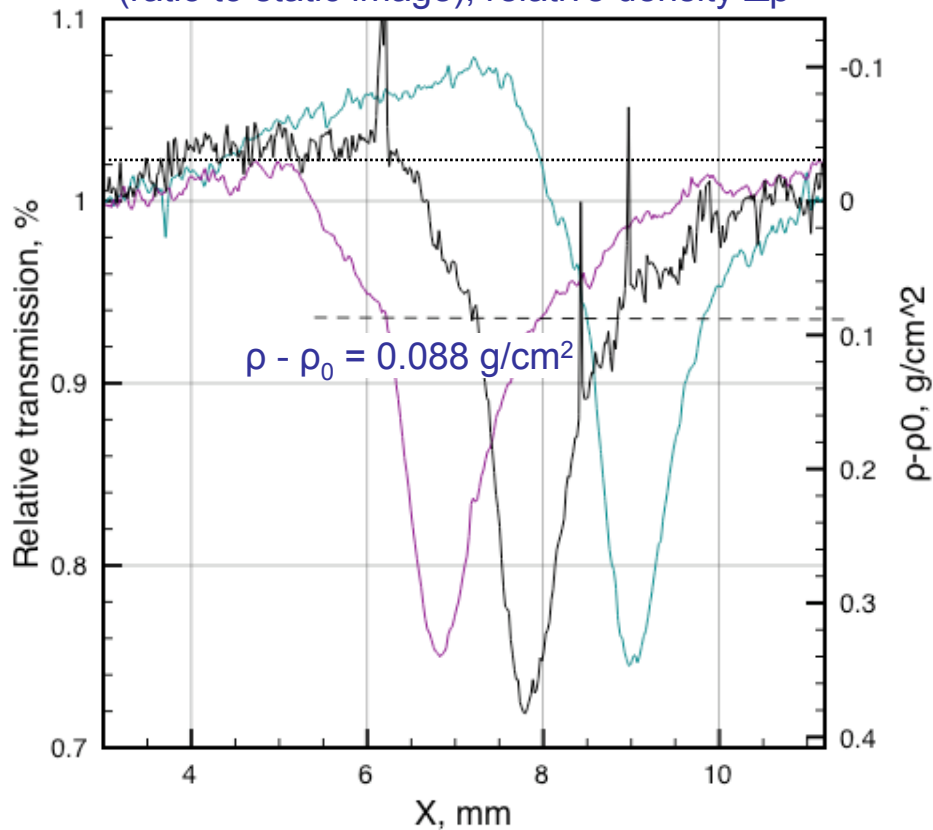
$$\rho_0 = 2.5 * 2.034 * 0.00589 = 0.03 \text{ g/cm}^2$$

Static image

# Shock Compression of Noble Gases

Xenon  $P_0 = 2.5$  Bar

Beam transmission for image profiles  
(ratio to static image), relative density  $\Delta\rho$

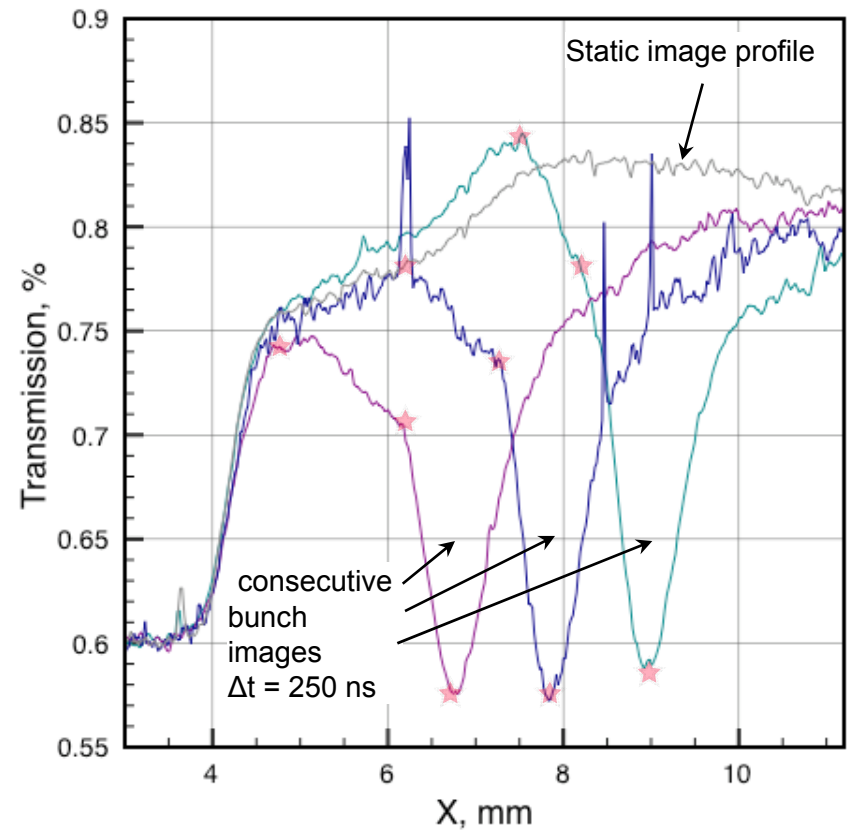


$$\Delta\rho - \rho_0 = 0.088 \text{ g/cm}^2$$

$$\rho_0 = 0.030 \text{ g/cm}^2$$

$$H \sim \frac{(\rho - \rho_0) d}{\rho_0 D \tau} + 1 = 9.38 \quad (d > D\tau)$$

Beam transmission for image profiles



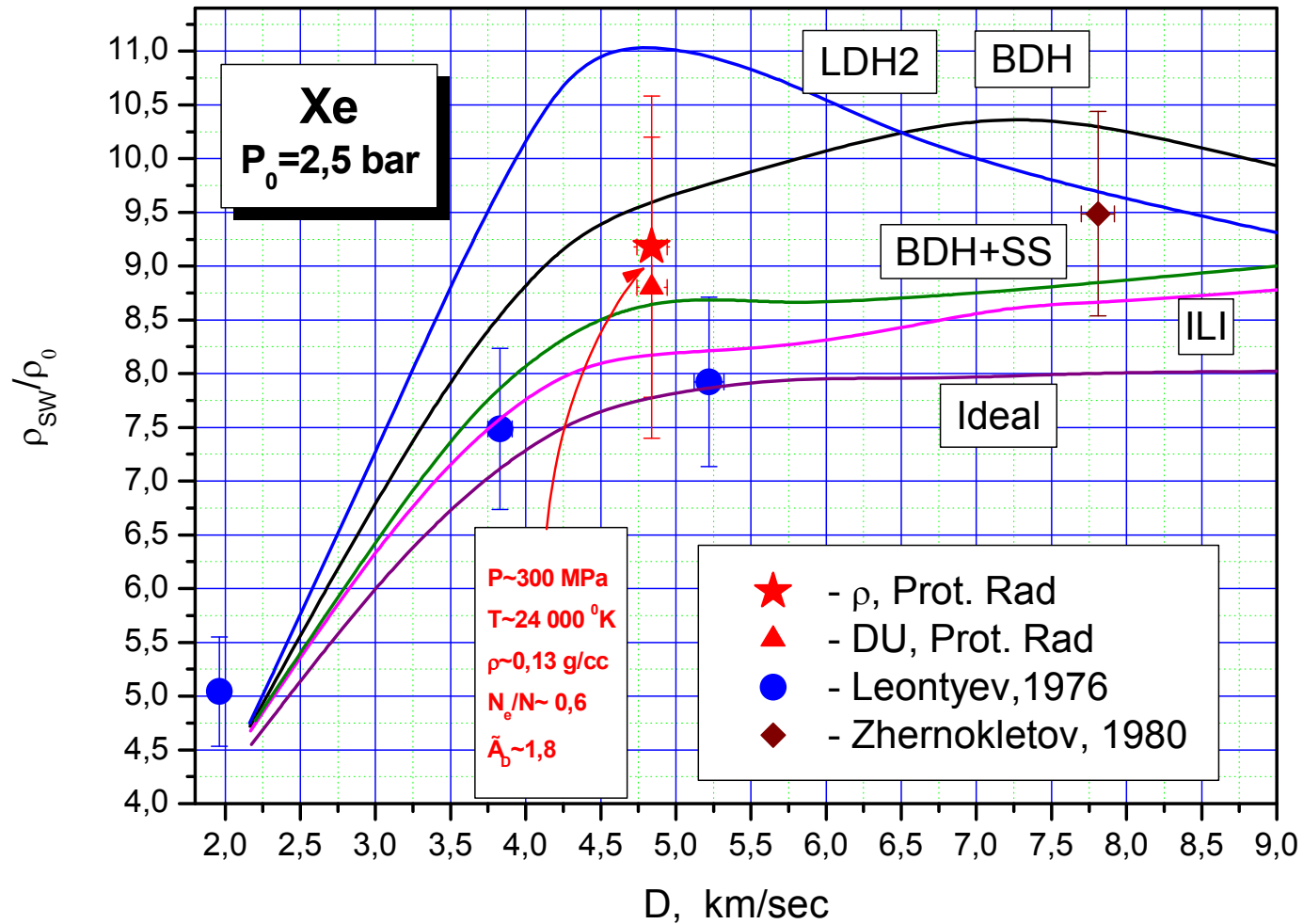
$$D = 4.84 \pm 0.09 \text{ km/s}$$

$$U = 4.29 \pm 0.09 \text{ km/s}$$

$$H \sim \frac{D}{D - U} = 8.8$$



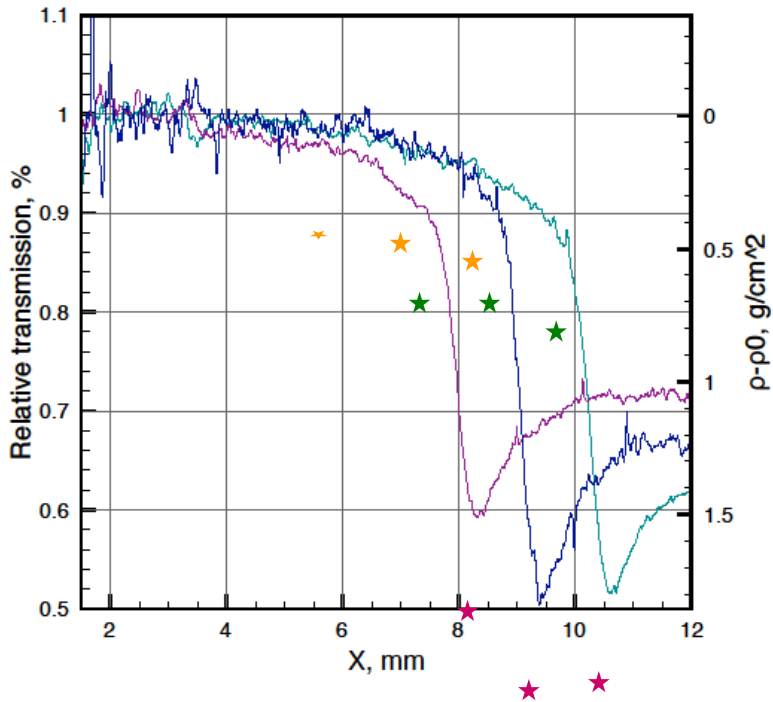
# Shock Hugoniot of Xenon at $P_0 = 2.5$ Bar



# Shock Compression of Noble Gases

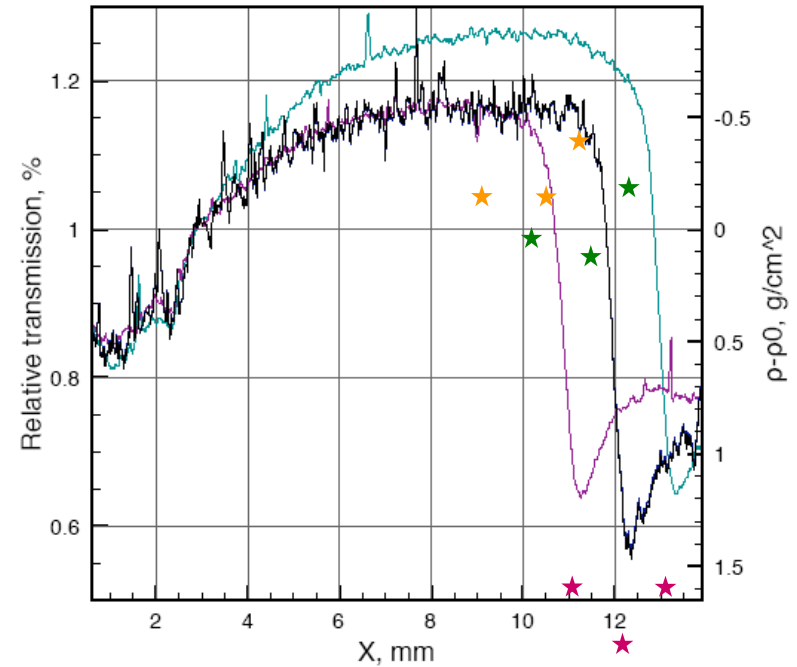
## Argon

$P_0 = 3.5$  Bar



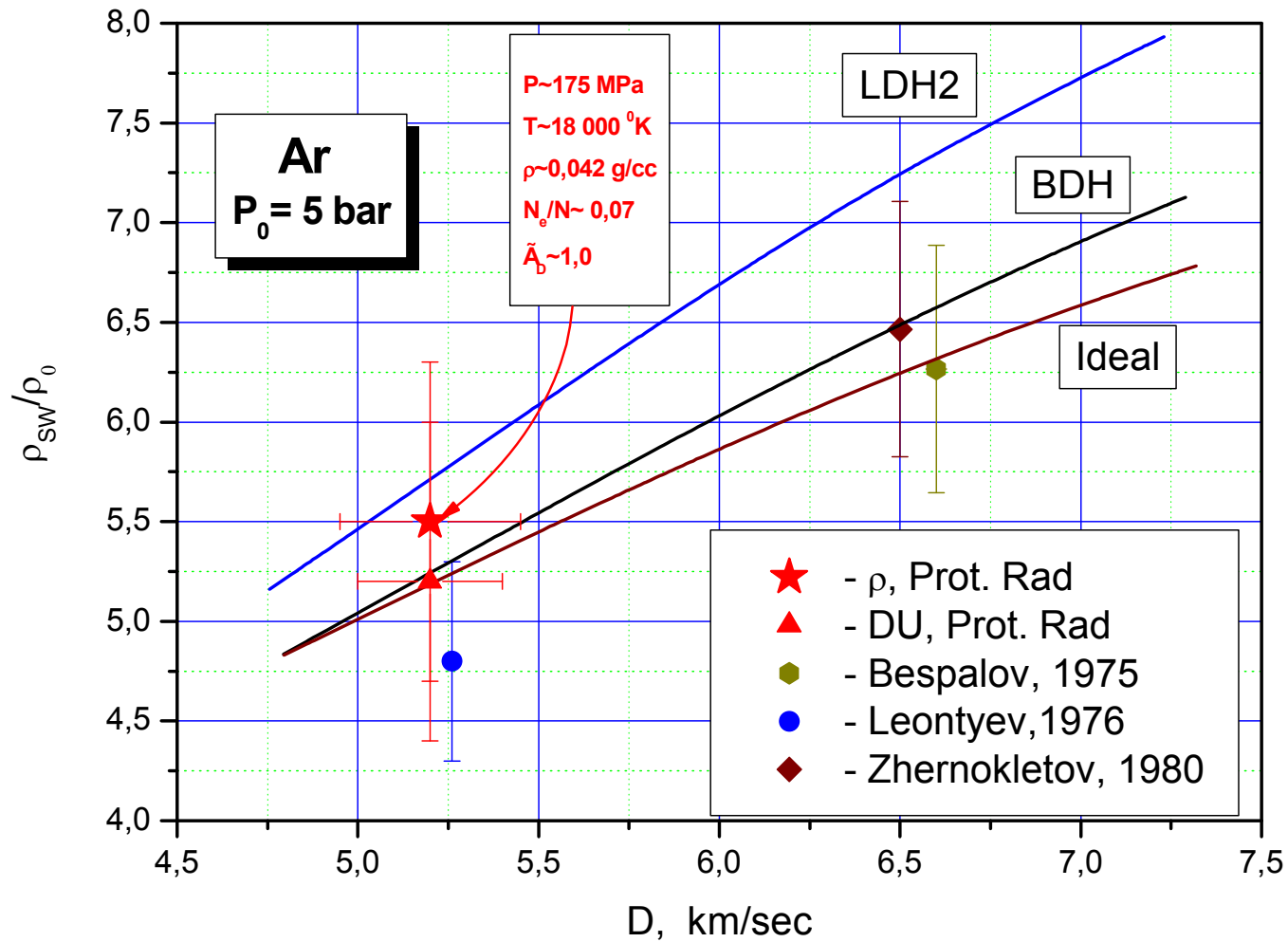
$D = 5.4$  km/sec  
 $U = 4.5$  km/sec

$P_0 = 5$  Bar



$D = 5.2$  km/sec  
 $U = 4.2$  km/sec

# Shock Hugoniot of Argon at $P_0 = 5$ Bar



# PRIOR Project

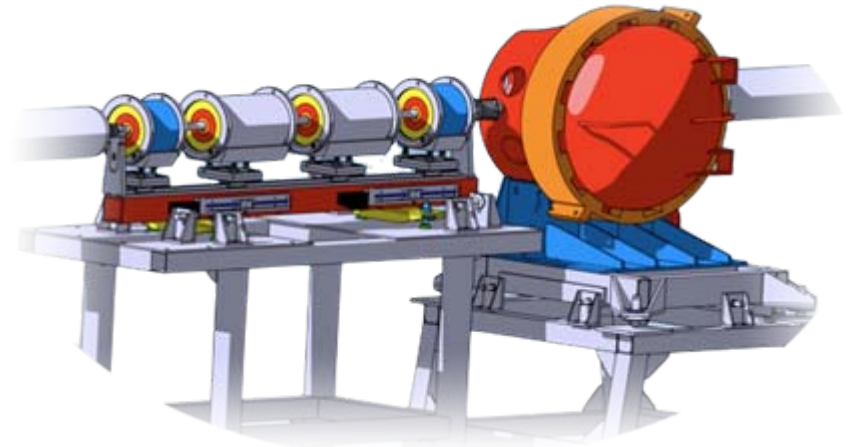
## PRIOR = Proton Microscope for FAIR

### 4.5 GeV Proton Microscopy:

- $5 \cdot 10^{12}$  protons from SIS-18 beam line in GSI (Darmstadt, Germany);
- **less than 10  $\mu\text{m}$**  spatial resolution;
- **sub-percent** density resolution;
- target areal density up to **5 – 50  $\text{g}/\text{cm}^2$** ;
- high-Z targets;
- temporal resolution **< 20 ns**;
- multi-frame capability

### ***Collaborators:***

- GSI Helmholtzzentrum für Schwerionenforschung (Germany)
- Technische Universität Darmstadt (Germany)
- Institute for Theoretical and Experimental Physics (Russia)
- Institute of Problems of Chemical Physics RAS (Russia)
- Joint Institute for High Temperatures (Russia)
- Los Alamos National Laboratory (USA)



# Conclusions

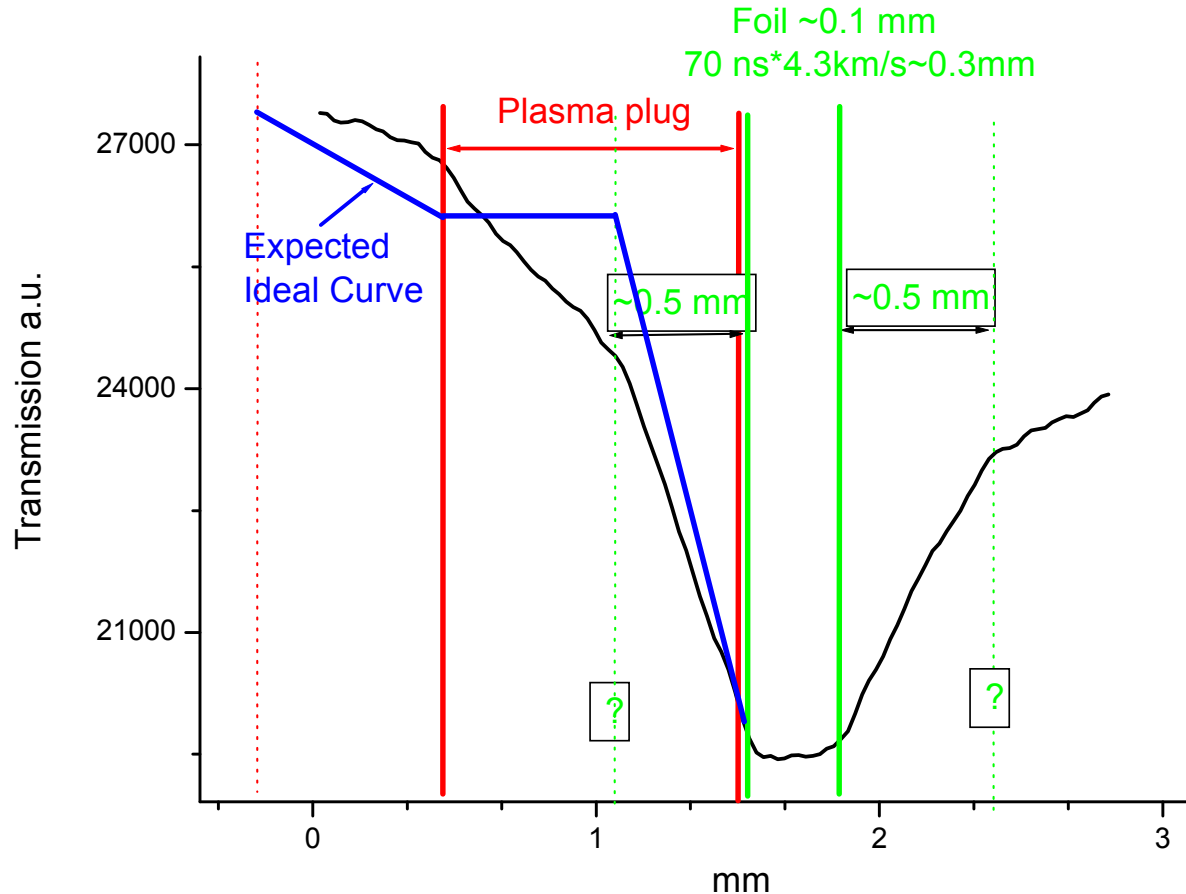
## Current fields of research at ITP-TWAC Proton Radiography Facility:

- Detonation of solid and emulsion explosives;
- Surface ejecta formation in metals under shock loading;
- Shock-compressed plasma of noble gases;
- Development of new compact explosive generators.

## What's Next:

- Phase transitions in shock-compressed materials (metals, liquid nitrogen...);
- Experiments with noble gases at higher initial pressures;
- Experiments with cryogenic targets;
- Development of PRIOR facility at GSI/FAIR.

# Transmission Profile for Xe at 2.5 Bar



Possible explanation : misalignment  $2.5^\circ$